A THESIS

On

ZINC SELENIDE NANOSTRUCTURES
&
EFFECT OF IMPURITIES

Submitted in the partial fulfillment of requirement for the award of the degree of

Master of Technology (M. Tech)

IN

MATERIALS SCIENCE AND ENGINEERING

Submitted by
NIDHI SHARMA
ROLL NO :6050505

Under the Guidance of
Dr.N.K.VERMA
Professor and Dean

School of Physics and Materials Science
THAPAR UNIVERSITY
PATIALA (PUNJAB)-147004

JUNE 2007

Dedicated

To

My Parents

CERTIFICATE

This is to certify that the thesis entitled **ZINC SELENIDE NANOSTRUCTURES & EFFECT OF IMPURITIES** submitted by **Ms. Nidhi Sharma** in the partial fulfillment of the requirement for the award of the degree of **M. Tech** in **Materials Science and Engineering** from the **School of Physics and Materials Science, Thapar University, Patiala,** is a record of candidate's own work carried out by her under my supervision and guidance. The matter embodied in this report has not been submitted in part or full to any other university or institute for the award of any degree.

(Dr. N.K.Verma)
Professor & Dean
School of Physics and Materials Science
Thapar University, Patiala-147004 (Punjab)

Countersigned by:

(Dr. O.P. Pandey)
Professor & Head
Thapar University
Patiala-147004 (Punjab)

(Dr. R.K.Sharma)
Dean, Academic Affairs
Thapar University
Patiala-147004 (Punjab)

Dated:

ACKNOWLEDGEMENT

The real spirit of achieving a goal is through the way of excellence and discipline.
I would have never succeeded in completing my task without the cooperation, encouragement and help provided to me by various personalities.

With deep sense of gratitude I express my sincere thanks to my esteemed and worthy supervisor **Dr. N.K. Verma,** Professor, School of Physics and Material Science, for his valuable guidance in carrying out this work under his effective supervision, encouragement, enlightens and cooperation.

I shall be failing in my duties if I do not express my deep sense of gratitude towards **Dr.O.P.Pandey**, Professor & Head, School of Physics and Materials Science, who has been a constant source of inspiration for me throughout this work.

My special thanks to **Dr.Sunil Kumar**, for his timely help, cooperation and useful discussions. I wish my heartfelt thanks to research scholors **Karamjit Singh , Zinki Jindal** and **Raminder Kaur** for their generous help and good wishes.

My project would not have seen daylight without the immense cooperation of all my friends specially **Simta** and **Kamal** who helped me at various stages during the due course of my work.

I owe my sincere thanks to all the staff members of **School of Physics and Materials Science** for their support and encouragement.

I am also thankful to **my husband** for his motivation and generous support. I would like to thank **my parents** for their moral support that kept my spirit up during the endeavor. My greatest thanks are to all who wished me success.

Above all I render my gratitude to the **ALMIGHTY** who bestowed self-confidence, ability and strength in me to complete this work.

(NIDHI SHARMA)

ABSTRACT

ZnSe is an important II-VI semiconductor and has been highlighted as an efficient emitter because of its high quantum yield and proper band gap in the visible range. PVP capped, pure and doped (Mn, Cu, Co) ZnSe nanoparticles (average diameter ~ 14 nm) have been synthesized using chemical precipitation technique in the aqueous media. The average particle size has been calculated using X-ray diffraction pattern and the Transmission Electron Microscopy (TEM) images. SAED pattern showed the crystalline nature of the synthesized material. Laser induced photoluminescence studies have been done to calculate various parameters like excited state lifetimes, emission wavelengths and trap depth values of the fabricated nanoparticles.

CONTENTS

CHAPTER 1

INTRODUCTION

1.1 Nanoscience and Technology

1.1.1. Introduction to nanotechnology

The greek word 'nano' is referred to the length scale of one billionth of a meter. Thus nanoscience deals with the science of materials and technologies in the scale range of ~ 1-100 nm. This means, the nanoscience deals with a few hundred to a few thousand atoms or atomic clusters, whereas the microscopic word is made out of trillion of atoms or molecules. Nanoparticles are larger than individual atom and molecules, but are smaller than bulk solid; hence they obey neither absolute quantum chemistry nor laws of classical physics and have properties that differ markedly from those expected. Presently, the nanoscience and technology represents the most active discipline all around the world and is considered as the fastest growing technology revolution in the human history had ever seen. This intense interest in the science of the materials confined within the atomic scales stems the fact that these nanomaterials exhibit fundamentally unique properties with great potential of bringing plethora of next generation technologies in electronics, computing, optics, biotechnology, medical imaging, medicine, drug delivery, structural materials, aerospace, energy etc.

1.1.2. Nanostructure materials

Nanostructured materials are materials with the characteristic length scale of the order of a few (typically 1 to 100) nanometers. The structure refers to the chemical composition, the arrangement of the atoms, and the size of a solid in one, two or three dimensions; effects controlling the properties of nanostructure materials include size effects (where critical length scales of physical phenomenon become comparable with the characteristic size of the building blocks of the micro structure), changes of the dimensionality of the system, changes of the atomic structure and alloying of components, e.g. elements that are not miscible in the solid and/or the molten state. The synthesis, characterization and processing of nanostructure materials are part of an emerging and rapidly growing field. Research and development in this field emphasizes scientific discoveries in the generation of materials with controlled micro structural characteristics. Nanostructured materials may be grouped under nanoparticles, nanointermediates, and nano composites. They may be in or far away from

thermodynamic equilibrium. For example nano-structured materials consisting of nanometer sized crystallites of Au or NaCl with different crystallographic orientation and chemical compositions vary greatly from their thermodynamic equilibrium.

Research in present day nanomaterials is based largely on the investigating fundamental properties of matter in nanoscale regime, however, the timely attention and efforts are essential for the transformation of these new findings into technology product so that the well assumed technology revolution will become day light reality. By now, a variety of chemical, biological as well as physical processes are established for the preparation of different kinds of nanoparticle systems and the ground breaking inventions such as scanning tunneling microscopy (STM), atomic force microscopy (AFM), etc, made the characterization and atomic scale manipulation of nanoscale materials a practical reality.

1.1.3. Semiconductor nanoparticles

Almost all materials system including metal, insulators and semiconductors show size dependent electronics or optical properties in the quantum size regime. Among these, the modification in the energy band gap of semiconductors is the most attractive one because of the fundamental as well as technological importance. Semiconductors with widely tunable energy band gap are considered to be the materials for next generation flat panel displays, photovoltaic, optoelectronic devices, laser, sensors, photonic band gap devices, etc. When dimension of a material is continuously reduced from macroscopic size to nanometers, the physical and chemical properties drastically change. If one dimension is reduced to nanometer range, so that the size is comparable to the de-Broglie wavelength of the exciton; while other two dimensions remain large, one obtains a structure known as quantum well. If two dimensions are reduced and one remains large, the resulting structure is referred as quantum wire. And if all three dimensions are reduced, the material is called a quantum dot. The word quantum is associated with these three types of the nanostructures because the change in properties arises from quantum mechanical nature of physics in ultra small domain. In, quantum dots, the surface to volume ratio is large and surface effects dominate.

Quantum dots, also known as nanocrystals, are a special class of materials, composed of periodic groups of II-VI, III-V, or IV-VI semiconductors. Semiconductors derive their great importance from the fact that their electrical conductivity can be greatly altered via an external stimulus (voltage, photon flux, etc), making semiconductors critical parts of many different kinds of electrical circuits and optical applications. Quantum dots are unique class of semiconductor because they are so small, ranging from 2-10 nanometers (10-50 atoms) in diameter. At these small sizes materials behave differently, giving quantum dots unprecedented tunability and enabling never before seen applications to science and technology. Optical properties of the quantum dots can be easily tuned with the particle size. The band gap can be controlled with the change in size of the nanomaterial, so the different colored emission can be observed from the same material. These quantum dots of same material can be used for fabrication of LEDs having emission over the whole visible spectrum.

The usefulness of quantum dots comes from their peak emission frequency's extreme sensitivity to both the dot's size and composition, which can be controlled using Evident Technologies' proprietary engineering techniques. This remarkable sensitivity is quantum mechanical in nature, and is explained as follows.

The electrons in quantum dots have a range of energies. The concepts of energy levels, band gap, conduction band and valence band still apply. However, there is a major difference. Excitons have an average physical separation between the electron and hole, referred to as the Exciton Bohr Radius, this physical distance is different for each material. In bulk, the dimensions of the semiconductor crystal are much larger than the Exciton Bohr radius, allowing the exciton to extend to its natural limit. However, if the size of a semiconductor crystal becomes small enough that it approaches the size of the material's Exciton Bohr radius, then the electron energy levels can no longer be treated as continuous - they must be treated as discrete, meaning that there is a small and finite separation between energy levels. This situation of discrete energy levels is called quantum confinement, and under these conditions, the semiconductor material ceases to

resemble bulk, and instead can be called a quantum dot. This has large repercussions on the absorptive and emissive behavior of the semiconductor material.

Fig.1-Quantum dot

1.1.4 Properties of Nanomaterials

In nanoparticles the properties (physical, chemical, biological etc.) can be selectively controlled by engineering the size, morphology, and composition of the particles. Nano materials are known to exhibit markedly different properties compared to micron sized ones. These new substances will have enhanced or entirely different properties from their bulk counterparts.

It has been shown that the various material properties such as electrical, mechanical, optical, magnetic etc are highly influenced by the fine-grained structure and their is generally improvement in the concerned properties. Using a variety of synthesis methods, it is possible to produce nanostructured materials in the various forms like: thin films, powder, quantum wires, quantum wells, quantum dots, etc. There is also considerable interest in the generation of carbon nanostructures, which are related to the famous Bucky ball. In addition, the use of nanosized materials as fillers for composite materials are generating interest ; specifically in the case of polymer nanocomposites. All materials are composed of grains, which in turn comprise many atoms. These grains are usually invisible to the naked eye, depending on the size. Conventional materials have grains varying in size any where from 100's of microns (μm) to millimeters (mm). A nanocrystalline material has grains on the order of 1-100nm. The average size of the atom is of the order of 1 to 2 A^0 in radius. One nanometer comprises of 10 Å, and hence

in one nanometer (nm) there may be 3-5 atoms, depending on the atomic radii. Nanocrystalline materials are exceptionally strong, hard, and, ductile at high temperature, wear-resistance and chemically very active. Nanocrystalline materials are also much more formable than their conventional, commercially available micron counterparts.

1.2 Luminescence

1.2.1 Introduction to Luminescence

Luminescence is the process where an electromagnetic radiation is produced by a substance under suitable external excitation. At certain frequencies, this radiation is significantly in excess of the thermal radiation, which is emitted by a substance at that particular temperature. The so-produced electromagnetic radiation, generally in the visible region, is characteristic of the particular luminescent material under examination, termed as phosphor [1]. The emission of visible light (400-700nm) corresponding to the region between red and violet requires excitation energies the minimum of which is given by Einstein's law stating that the energy, E, is equal to Planck's constant, h, times the frequency of light, ν, or Planck's constant times the velocity of light, c, in a vacuum divided by its wavelength, λ, that is:

$$E = h\nu = hc/\lambda.$$

If the emission energy is less than the excitation energy, the emission is known as 'Stokes emission', and, if the emission energy is greater than the excitation energy, the emission is known as 'Anti-Stokes' emission. Generally Stokes emission is observed because the difference in energy is caused by the transformation of the exciting light, to a greater or lesser extent, to non-radiating vibration energy of atoms or ions.

Depending on how the phosphor is excited, several types of luminescence processes are distinguished from each other as follows:

Type	Source of excitation
a) Photoluminescence	Electromagnetic radiation
b) Cathodoluminescence	Electrons
c) Electroluminescence	Stationary/varying electric field
d) Chemiluminescence	Chemical reactions
e) Bioluminescence	Biological process
f) Sonoluminescence	Acoustic energy
g) Triboluminescence	Mechanical energy
h) Thermoluminescence	Temperature changes
i) Radioluminescence	Subatomic particles

a. Photoluminescence

Photoluminescence, which occur by virtue of electromagnetic radiation falling on matter. The emissions are generally in the visible part of the spectrum. It has been shown that, in luminescence caused by light, the wavelength of emitted light generally equal to or longer than that of exciting light (i.e. of equal or less energy).

b. Cathodoluminescence

Cathodoluminescence occurs when the system is excited by means of electrons and the emission generally is in the visible region. Among the various kinds of luminescence, that excited by cathode rays would appear to have been the subject of most practical applications in recent years, e.g. cathode ray tubes for oscilloscopes, monochrome, colour television, radar etc

c. Electroluminescence

The term Electroluminescence includes several distinct phenomena, a common feature of which is that light is emitted by an electric discharge in gases, liquids, and solid materials. In 1752, Benjamin Franklin, identified the luminescence of lightning as caused by electric discharge through the atmosphere. The Electroluminescence sometimes observed at electrodes during electrolysis is caused by the recombination of ions (therefore this is sort of Chemiluminescence). The application of an electric field to thin

layers of luminescent Zinc Sulfide can produce light emission, which is also called Electroluminescence.

d. Chemiluminescence

Most of the energy liberated in chemical reactions, especially oxidation reactions, is in the form of heat. However, in some reactions, part of the energy is used to excite electrons to higher energy states, and for fluorescent molecules, Chemiluminescence results. Studies indicate that Chemiluminescence is a universal phenomenon, although the light intensities observed are usually so small that sensitive detectors are necessary to detect it. There are some compounds that exhibit brilliant Chemiluminescence, the best known being luminol, which when oxidized by Hydrogen Peroxide, can yield a strong blue or blue greenish Chemiluminescence.

e. Bioluminescence

Bioluminescence is a special type of Chemiluminescence catalysed by enzymes. The light yield of such reactions can reach 100 percent, which means that almost without exception every molecule of the reacting luciferin is transformed into a radiating state. All of the bioluminescent reactions best known today are catalyzed oxidation reactions in the presence of air.

f. Triboluminescence

When crystals of certain substances, e.g. sugar are crushed, luminescent sparkles are visible. Similar observations have been made with numerous organic and inorganic substances. Closely related are the paint blue luminescences observable when adhesive tapes are stripped from a roll, and luminescence exhibited when Strontium Bromate and some other salts are crystallized from hot solutions.

g. Sonoluminescence

Sonoluminescence occurs when the system is excited by means of ultrasonic waves. Ultrasonic waves are elastic waves which have a frequency greater than 20 kHz. These waves are also known as inaudible sound waves.

h. Thermoluminescence

Thermoluminescence means not temperature radiation but enhancement of light emission of the materials already excited electronically by the application of heat. This phenomenon is observed with some minerals and, above all, with crystal phosphors after these have been excited by light.

i. Radioluminescence

Radioactive elements can emit alpha particles (helium nuclei), electrons, and gamma rays (high-energy electromagnetic radiation). The term Radioluminescence, therefore, means that an appropriate material is excited to luminescence by a radioactive substance. When alpha particles bombard a crystal phosphor, tiny scintillations are visible to microscopic observation. Self-luminous paints, used for dial makings for watches and other instruments, owe their behavior to Radioluminescence.

As regard to the mechanism of luminescence, phosphors may be classified into two groups. In the first group are those substances (in general, organic compounds) in which luminescence are associated with the molecules of the particular substance. Upon absorbing the excitation energy, the molecules undergo transition to an excited energy state, emit radiant energy and then returns to the ground state.

The second group of phosphors comprises materials (in general inorganic compounds) in which luminescence is related to their crystal structures and vanishes when those structures are destroyed. Perturbations in the periodic structures of a crystal lattice or the presence of foreign atoms or ions in the lattice constitute the condition for the luminescence to occur. Such atoms, called activators [2], exhibit the ability to absorb the excitation energy and are ionized in the process. After sometime the free electrons recombine with the ionized activators and energy is radiated in the form of electromagnetic radiation.

Luminescence is further subdivided into *fluorescence* and *phosphorescence.* A molecule in an excited state radiates energy after remaining in a metastable state for a fairly long time; the process is termed as phosphorescence.

The luminescence process in which the molecule emits radiation as it falls directly from an excited state to a lower energy state is known as fluorescence. The time scale of the process is of the order of 10^{-8} s. Fluorescence radiation is due to allowed transitions ($\Delta S = 0$) from singlet excited state to the singlet ground state.

If a molecule in an excited state radiates energy after remaining in a metastable state for a fairly long time, the process is termed as phosphorescence. The time scale of the phosphorescence process depends on the energy spacing between the metastable state and the nearest energy state to which transition is allowed and may be of the order of 10^{-6} second to minutes, hours or even days. This type of transition is due to forbidden transition ($\Delta S \neq 0$) from the excited metastable state to the lower ground state

1.2.2 Origin of Fluorescence and Phosphorescence

The absorption of energy by a molecule raises it to an excited state. This excited state may be rotational, vibrational or electronic, depending upon the energy of exciting photon. If the energy of the exciting photon is of the order of 10^{-3} eV the rotational states can be excited, if the energy is of the order of 0.1eV then vibrational states can be excited, and if the energy is of the order of several electron volts then electronic states can be excited. The corresponding spectra are in microwave for rotational, infrared for vibrational and visible as well as ultraviolet range for electronic energy states.

A molecule in an excited electronic state can loose energy and return to its ground state in a number of ways. The molecule may come to the ground state by the emission of a photon of same energy in a single step.Another possibility is, that it may loose some of its vibrational energy in collision with other molecules. Therefore downward radiative transition originates from a lower vibrational level in the upper electronic state. This

phenomenon is called fluorescence and the fluorescent radiation is always of lower frequency Fig. 3 (a).

In molecular spectra, radiative transitions between electronic states of different total spin are prohibited (spin selection rule $\Delta S = 0$). Fig. 1.1(b) shows a situation in which a molecule in its singlet (total spin quantum no. S = 0) ground state, absorbs a photon and is raised to singlet excited state. In collisions the molecule can undergo radiationless transitions to a lower vibrational level. Now, lower vibrational level may have the same energy as one of the triplet (S = 1) excited state. There is then a certain probability of the molecule for a shift to occur to a triplet state. Further collisions in the triplet state bring the molecule's energy below that of the crossover point, so that it is now trapped in the triplet state and ultimately reaches v = 0 level.

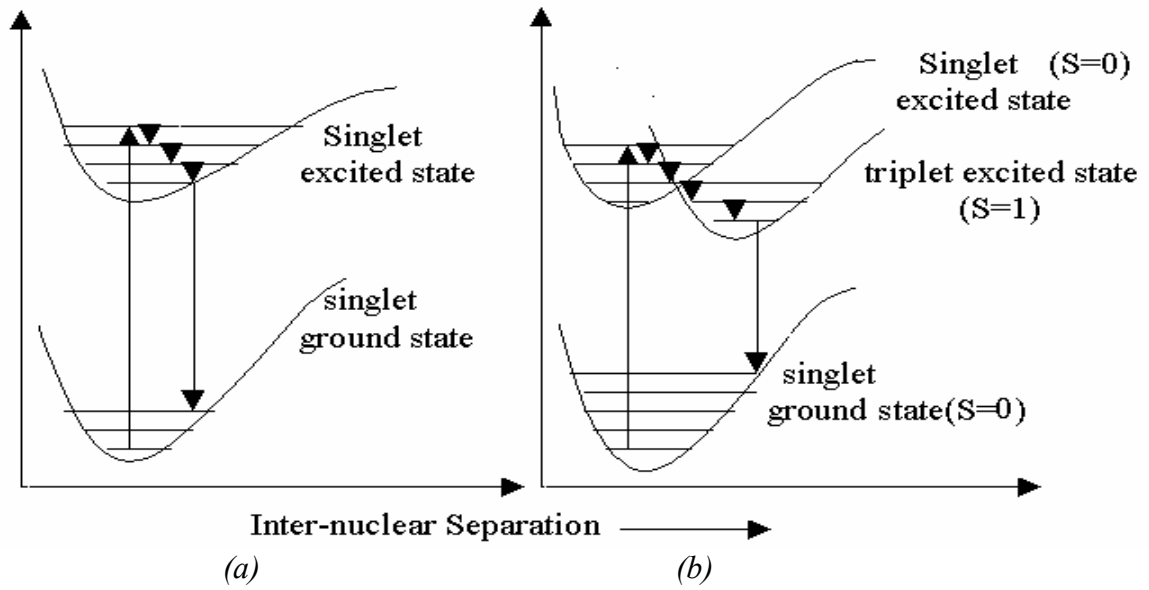

Fig.2-(a) origin of fluorescence (b) origin of phosphorescence

As the radiative transition from a triplet to a singlet state is forbidden($\Delta S \neq 1$) by spin selection rule, which means not that it is impossible but that it has only a small likelihood of occurring. Such transitions have long lifetimes, and the resulting phosphorescent radiation may be emitted in the time interval of the order of seconds, minutes or even hours after the initial excitation is switched off.

The name luminescence has been accepted for all light phenomena not caused solely by a rise of temperature, but the distinction between the terms phosphorescence and fluorescence is still open to discussion. With respect to organic molecules, the term phosphorescence means light emission caused by electronic transitions between levels of different multiplicity whereas the term fluorescence is used for light emission connected with electronic transitions between levels of like multiplicity. The situation is far more complicated in the case of inorganic phosphors.

1.2.3 The General Characteristics and Applications of Phosphors

A phosphor is defined as a substance which posses the property of luminescence. This concept generally refers to a certain group of solid materials doped with certain amount of activators or impurities. These phosphors find most extensive applications as a source of light stimulated by other kinds of energy. The applications [3] of phosphors lend themselves to classification under three main headings:

A. Illumination – fluorescent lamps; excited by means of ultraviolet radiation.
B. Radiology - the screen films of x–ray machines excited by x-rays.
C. Data transmission – screens of television picture tubes, radar sets, cathode ray oscilloscopes, computer monitors, electron microscopes, and image converters; stimulated by an electron beam.

Fluorescence excited by means of ultraviolet radiation has many applications such as in fluorescent lamps, to help identify minerals and biochemical compounds. In a fluorescent lamp, a mixture of mercury vapor and an inert gas inside a glass tube gives ultraviolet light when excited by an electric discharge. The tube is coated with phosphorescent material from inside, which gives visible light when excited by ultraviolet radiation. This process is much more efficient than using a current to heat a filament to get electromagnetic radiation in the visible region, as in an ordinary light bulb.

The phosphors used for these purposes are inorganic compounds. They are most frequently sulfides and oxides or silicates and phosphates of such metals as zinc, calcium, magnesium, cadmium, tungsten and zirconium. Small amounts of (0.01-1%) of metal impurities are added to serve as activators or dopants to get the visible colours of emitted radiations.

Phosphors, most frequently in the form of fine crystals, are deposited in the form of a thin layer on a suitable base, usually glass, to produce a luminescent screen, which is excited by an electron beam to produce visible radiation as in case of screens of TV picture tubes, CRO, computer monitors, electron microscopes and image converters.

1.2.4 Luminescence of Doped II-VI Semiconductor Chalcogenide Phosphors

Light emission from nanocrystalline phosphors is possible through a radiative recombination process of charge carriers generated by higher energy photon absorption. The colour of the emission can be tailored by changing the crystalline size and appropriate doping. Recently, doped semiconducting nanocrystals (NC) have attracted considerable interest due to their interesting properties such as high luminescence quantum efficiency, short radiative lifetime , size dependent emission color tunability , low voltage cathodoluminescence , multicolor electroluminescence etc. These materials are considered to be the luminophors for next generation displays, bio-labels, lasers, etc.

ZnS and CaS phosphors doped with various activators are very attractive luminescent materials used in variety of applications such as screens of cathode ray oscilloscopes, fluorescent lamps, television picture tubes, cameras and radars. Besides these direct applications of the luminescence of these phosphors certain indirect applications of these phosphors have also been recently reported. Karvets [4] has reported CaS doped with Sr and Ce as an optical memory storage material having erasable and re-writeable memory. Khare et al [5] have reported CaS:Cu as a temperature sensor. Due to extensive applications of these phosphors, the luminescent properties of these phosphors had been investigated by large number of workers [6-7] with different concentration of

activators and co-activators. Different concentration of a dopant gives different result in the same host lattice. The decay of luminescence in these phosphors is primarily determined either by the electron transition within the activator ion or by carriers temporarily captured in various trapping states depending upon which is slower. Since the traps are always present in these phosphors, the phosphorescence decay even with relatively fast activator ions is slower than might be desired for some applications of particular interest. In the present case singly doped phosphors as well as multiple doped phosphors are studied. Also the effect of killer impurities (Fe, Co, Ni) on the luminescence of these phosphors is studied, as a parameter of concentration of the activators.

1.2.4.1 Types of Centers, Activators & Co-Activators in Phosphors

Various types of centers, activators & co-activators are involved in the luminescence process and various models are suggested for the explanation of the luminescence phenomenon occurring in the inorganic phosphors. There are three types of centers involved in the luminescence process and they are given below:

a) Centers near to the Conduction Band: These centers are simply deeper than typical electron traps, and transitions to the valence band although less probable than those from the conduction band to these centers still have an appreciable probability. This model was postulated by Lambe and Klick. First of all, a conduction electron is captured in the localized level and then this electron falls in to a hole in the conduction band. This last transition gives radiative emission in the visible range.

b) Centers near to the Valence Band: This is the classical model for copper centers in Zinc Sulphide postulated by Riehl, Schon and Klasens. Copper produces a level in the forbidden energy band several tenths of an electron volt above the valence band which has a high probability for positive hole capture (it is assumed that a hole diffusing through the valence band is immediately captured by the center when hole lies below it). The center also is allowed a significant capture probability for conduction electrons, and

this gives rise to luminescence as observed by a transition to the center's ground state from the bottom of the conduction band.

c) Centers involving a Ground State near the Valence Band and an Excited State near to the Conduction Band: After the discussions given above it is clear that the levels near the ground state have a high hole capture probability and the levels near the conduction band have a high electron capture probability. After the capture has taken place in each type, emission can take place by a transition of the electron from the upper level to the lower level. The only condition is that the temperature is not too high, so that electrons are not freed by thermal activation from the levels, below the conduction band. This model is known as William-Prener model.

Activators are used for creating the luminescent centers in the host phosphor material .These itself act as a luminescent centers or perturbate the localized levels which are already there due to imperfections in the host crystal. The fluxes (e.g Sodium Chloride) act as co-activator by facilitating the incorporation of the activator ions. The co-activators are known as charge compensators and they reduce the temperature required for the preparation of the phosphor appreciably.

In describing a luminescent phosphor, the following information is pertinent: crystal class and chemical composition of the host crystal, activator (type and percent), co-activator, temperature and time of crystallization process, emission spectrum and persistence.

An important condition of getting highly efficient phosphors is that the sulfides and selenides must be prepared to the highest possible chemical purity before the necessary amount of activator can be added precisely. ZnS, CdS and ZnSe phosphors are especially efficient in electroluminescence. Phosphors are produced from pure Zinc Sulphide and Calcium Sulfide or their mixture by heating them together with small quantities (0.1 - 0.001 percent) of copper, silver, Gallium, or other salts (activators) and with about 2 percent of sodium or another alkali chloride at about 1000°C. The role of the

alkali hallides is to facilitate the melting process and, above all, to serve as co-activators (fluxes). Only small quantities of the alkali halide are integrated into the phosphor, but this small quantity is highly important for its luminescence efficiency. Copper activated Zinc Sulphide and Cadmium Sulfide exhibit a rather long afterglow when their irradiation has ceased, and this is favourable for application in radar screens and self-luminous phosphors.

1.2.5 Time resolved spectroscopy

A wide variety of spectroscopic techniques have been employed by scientists to probe the static and dynamic processes occurring in complex molecular systems. The generations of extremely short and intense laser pulses have opened the new way for the study of fast transient phenomena such as energy transfer, energy storage, excitation and de-excitation processes in optical materials. A new field of laser spectroscopy is the time-resolved spectroscopic technique in which the detection of these transient phenomena is being done by using short and intense laser pulses. Time- resolved spectroscopy employing laser excitation is a very convenient method for analyzing optical materials in the ultra short time domain. It provides an insight into various atomic and molecular processes, which occur in the materials in the nanosecond and sub-nanosecond time regime. The relaxation parameters associated with various optical transitions reflect the atomic and molecular processes going on in these materials and their environment. Many physical and chemical properties influencing the optical transitions can be investigated by nanosecond time-resolved spectroscopy techniques [8]. Prior to the discovery of ultra short laser pulses, time- resolved spectroscopy of luminescent materials was confined to the use of mercury vapor lamp and other UV-lamps as the excitation sources. These sources had to be switched off manually or electrically for study of luminescence decay measurements. So these studies were limited to long period decays only. However, the advent of lasers made it possible to automatically investigate the ultra fast processes occurring during the excitation and de-excitation of atomic and molecular states. The population decay times and phase decay times of these coherently excited states can be studied with extremely high resolution under laser excitation.

The spectral resolution of most time-resolved techniques is in principle limited by the Fourier limit, $\Delta\nu = a / \Delta T$, where ΔT is the duration of short light pulses, and, a, depends on the pulse profile. In general, the spectral bandwidth,$\Delta\nu$, of laser pulses is much narrower than the bandwidth of pulses from incoherent light sources. Some time-resolved methods based on regular trains of short pulses even circumvent the Fourier limit,$\Delta\nu$ of a single pulse and simultaneously reach extremely high spectral resolution.

1.2.6 Generation and use of Short Laser Pulses

The behaviour of the laser output viz., the pulse duration, frequency, etc. strongly depends on the time scale of relaxation processes. If these parameters are slow, the induced emission drives the population inversion even below the threshold and the laser output discontinues until the pump has reproduced sufficient population inversion to start emission again. This results in “laser spiking ", here typical pulse width is of the order of a few microseconds. On the other hand, if relaxation processes are sufficiently fast, these rapidly damp the oscillatory fluctuations of the population inversion and a steady-state inversion is reached which is equal to the threshold inversion. In such cases the laser output follows the pump pulse. In the case of "self terminating" lasers, whose lower laser level has a longer lifetime than the upper level, the duration of laser pulses is limited by the slow depopulation rate of the lower level, and the laser emission may stop even before the pulsed pump drops below the initial threshold. As an example in case of Nitrogen laser [9] which is pumped by a fast transverse electrical gas discharge, the output laser pulse duration was reported to be of the order of 1-10 ns with typical peak powers of 0.1-1 MW.

Dye laser pumped with these Nitrogen $_{laser}$ pulses yield light pulses of tunable wavelengths with a pulse width of a few nanoseconds, peak powers of 1-100 kW, and repetition rate of 1 kHz. With different dyes covering spectral range between 0.36 and 1.2 μm. In order to get high time resolution, vacuum-ultraviolet (VUV) region, excimer lasers are widely used. It can produce VUV pulses with tunable wavelengths having nanosecond pulse width and MW peak power.

The sub-nanosecond range in time resolution can be obtained by the mode-locking techniques [10]. Some of the commonly used mode-locking techniques are active mode-locking, passive mode-locking and synchronous mode-locking. When a CW-laser is mode locked, its average output power decreases whereas the peak power increases. For example, in case of an argon-ion laser, the spectral width of gain-profile above threshold for one of the laser transitions is about 7 GHz which implies that pulse width of about 150 ps can be theoretically expected from such a CW mode-locked laser.

For dye lasers the spectral width of gain-profile is very large and is of the order of 3×10^{13} s^{-1}. With such a high spectral width, a pulse width of about 0.3×10^{-13} s should be possible. Such pulses are known as sub-picosecond laser pulses. Passive mode-locking [11] is the major technique for producing ultra short laser pulses in pulsed lasers. In this technique, a suitable saturable absorber (e.g., crypto cyanine dye) is used in place of the acousto-optic modulator along with active medium inside the resonator. Due to the saturation of absorber the intensity peaks bleach the absorber more than the average intensity loss. The saturation absorption coefficient decreases with intensity. The peaks of the fluctuation intensity, therefore, suffer fewer losses and will be amplified rapidly than the average intensity. After several round trips, this lead to the generation of ultra short and high power peak pulses. The passively mode-locked Nd:glass laser generates pulses in the 5 to 15 ps time range with extremely high peak power ($\geq10^{10}$ W) at λ=1.06 μm. A very efficient way of achieving a regular train of ultra short pulses from CW-Dye laser is synchronous mode-locking; an elegant way to produce mode-locked pulses with variable repetition frequency is to use a cavity dumping system [12]. Such a laser which combines both mode-locking and cavity dumping is known as a "combo laser" [13].

1.2.7 Lifetime Measurements with Lasers

Various techniques of producing short laser light pulses with variable wavelengths, time duration and repetition rates, allow the time-resolved spectroscopic measurements of the decay of selectively excited atomic, ionic or molecular levels. The most commonly used experimental techniques of lifetime measurements are phase-shift method, time-of-flight method, the pulse-excitation method and the technique of delayed

coincidence with single-photon counting technique. A brief account of these techniques with their merits and demerits is given in the following four sections. Since the pulse excitation technique is employed for the experimental investigations, a more elaborate description of this technique is given.

1.2.7.1 Phase Shift Method

Here the intensity I_{exc} of the incident light which excites the molecular level E_i is sinusoidaly modulated at a frequency,ω which is assumed to be small compared with the frequency, ω_{ik}. The exciting light intensity is given by:

$$I_{exc} = I_0(1+a \sin \omega t) \cos \omega_{ik} t \qquad (2.1)$$

The modulation is achieved by Pockel's cell or an ultrasonic light modulator. The fluorescence intensity, $I_{Fl,}$ is observed perpendicular to the incident light beam and is given by:

$$I_{Fl} = bI_0\left(1+\frac{a}{\sqrt{1+\omega^2\tau^2}}\sin(\omega t+\phi)\right)\cos\omega_{ik}t \qquad (2.2)$$

where a and b are proportionality constants.

This equation shows that the fluorescence intensity is modulated at the same frequency,ω, of the exciting light, but the modulation amplitude has decreased and its phase is shifted by ϕ against the modulation phase of $I_{exc.}$ The effective lifetime τ is given by:

$$\tau=1/(\rho B_{ik}+A_{ik}) \qquad (2.3)$$

And the relation between the phase shiftϕ, ω and τ is given by:

$$\tan\phi=\omega\tau \qquad (2.4)$$

Here ρ, B_{ik} and $A_{ik\ represent}$ the energy density of incident radiation and Einstein's coefficients for induced and spontaneous transitions from the initial level i to the final level k.

If $I_{exc} = c\rho_{exc}$ (where c is velocity of light) is sufficiently small, the induced emission term can be neglected and the extrapolation to $I_{exc} \longrightarrow 0$ yields the spontaneous lifetime $\tau_I = 1/\Sigma_k A_{ik,}$ if collisions are negligible. The effect of collisions on τ can be determined by plotting $1/\tau$ against the pressure (Stern-Vollmer plot), which yield at low temperature a straight line. The extrapolation to zero pressure gives the unperturbed spontaneous lifetime of the excited level of the free molecule. The phase shift method is not very well suited for the measurement of non-exponential decays. Another disadvantage of phase shift method is the influence of the induced emission, which is handicap especially when using laser for excitation. Also low signal- to- noise ratio at low intensities limits the accuracy of this method.

1.2.7.2 Time-of-Flight Method

This method uses fast atomic, molecular or ion beam with kinetic energies in the keV to MeV range. The atoms which move in the x-direction are excited at a well defined small interval Δx around x = 0. The excitation sources may be a laser or collisions with other atoms in foils or gas chambers. The subsequent fluorescence, $I_F(x)$, is measured as a function of distance x from the point of excitation. The transformation to a time scale $I_{Fl}(x)$ uses the relation x = vt where the velocity $v = (2eU/m)^{1/2}$ of the ions is measured by the acceleration voltage U and the mass of the ions. Neutral atoms and molecules can be produced from the ions by charge exchange. The accuracy of the method is in principle limited only by the accuracy of the distance measurement and many lifetime values of the highly excited atoms or ions have been measured by this method. A severe drawback of this method is the effect of cascade transitions on the measured decay curves. However this problem can be remedied by selectively exciting the levels using a tunable laser.

1.2.7.3 Single-Photon Counting Method

The single-photon counting technique is based on the concept that the probability distribution for the emission of a photon following an exciting pulse is identical to the intensity-time profile of the cascade of all the photons which are emitted following a single flash of exciting radiation. The single-photon probability distribution is built up by the repetitive exposure of the sample to the short laser bursts of the exciting radiation and recording the time of arrival of the first fluorescence photon following each exciting pulse. If more than one fluorescence photon arrives at the cathode of the photomultiplier following an excitation flash, only the first photon will be recorded because only one fluorescence photon stop pulse can be processed at the time-to-pulse height converter (TPHC) or the time-to-amplitude converter (TAC) per excitation start pulse. The interference of the later fluorescence events will distort the recording of the probability distribution by artificially enhancing the early portion of the fluorescence spectrum. This problem, usually associated with long decay times (pulse pile-up) originates from time-to-pulse height converter. Once a stop pulse has arrived within the preset time window, the time-to-pulse height converter cannot detect a second stop pulse in the same time window.

Pulse pile-up can be removed by suppressing measurements in which multiple stop pulses occur. A number of techniques are available for the rejection of pulse pile-up [14]. The simplest method for the prevention of the multiple photon events is to attenuate the light intensity reaching the photomultiplier. A practical value of the 10% of the incident intensity is taken for this purpose. Under these circumstances the multiphoton contribution will result in the distortion of only a few percent of any ratio of the stop to start frequency, which can usually be tolerated. The method has a disadvantage that the time required to record the spectrum increases due to the limited rate of data collection process.

Another basic problem associated with the recording of the single photon pulse is the interference of the dark pulse distribution in the photomultipliers. Most of the photomultipliers exhibit dark pulses, which have a pulse height distribution that differs

from that of the single photoelectron. Hence, it is necessary that if the photomultipliers are used for the photon counting, the electrical counting circuit of the photomultiplier tube output should not accept dark pulses. In order to achieve this output from the photomultipliers are supplied to discriminators which cut off dark pulses and pass photoelectron pulses having height greater than some pre-assigned value.

If the measured single exponential decay time is comparable to the instrumental response time (pulse-width of excitation pulse), the analysis consists of fitting a straight line to the natural/common logarithm of each channel count versus channel number determining the slope of the line. However, if the desired decay time is of shorter duration than the pulse width of the excitation source, significant distortion of the experimental data occurs because of the finite pulse duration than the pulse width of the light source, finite time spread of the photomultiplier and also finite time of the associated electronics. In such cases, the fluorescence data can be analyzed by the least square fitting method of moments or the convolution and deconvolution techniques [15].

1.2.7.4 Pulse-Excitation Method

In this method the molecules are excited by a light pulse with a trailing edge short compared to mean lifetime,τ, of the excited level. The subsequent population level decay, monitored by the decay of fluorescence intensity, is either viewed directly by a scope or is monitored with a boxcar integrator or a transient recorder. This method does not suffer from the influence of induced emission since the exciting light is already switched off when the fluorescence is being observed. Here, pulsed or mode locked lasers are usually used as the excitation sources. From the decay curve mean lifetime can be obtained directly. Any deviations from exponential decays can be seen immediately. The accuracy is comparable to the phase shift method. In general, the signals are detected in an analog form and many fluorescence photons per excitation pulse are required to obtain a sufficiently large signal-to-noise ratio.

1.3 Review of Literature

In 1945 Randal et al. [16] had studied phosphorescence and electron traps of various inorganic phosphors such as ZnS and CaS. They had reported long lifetime of the excited states in the order of minute-duration and assumed trap distribution to be uniform within the band gap of the semiconductors. They had also studied glow curves of these phosphors at room-temperature. In 1950, Bube [17] had studied luminescence and trapping states of undoped and Cu-doped ZnS phosphors. He reported blue and green luminescence in the phosphor with different concentration of copper impurity. He also reported trap–depths of the order of 0.89 to 1.00 eV in the energy band of the host phosphor. In 1961, Avinor et al had studied the nickel activated CaS and SrS phosphors. They had found that nickel impurity in these phosphors give very weak luminescence effects. In 1974, Jain et al. [18] had studied the decays and thermo luminescence of triply activated CaS phosphors. Triple activators used were Mn, Ce and Sm. They had shown the trap-depths of the order of 0.52 to 0.69 eV. In 1982, Bhatti et al. [19] had used laser as excitation source to study the photoluminescence of doped ZnS and CaS phosphors. The studies have been carried out at room temperature and liquid nitrogen temperature. At room temperature the lifetime values are in the range of 0.80 to 115.00 microsecond for CaS phosphors while in case of ZnS phosphors, the lifetime values are in the range of 0.87 to 23.12 microsecond. But the lifetime values were found to be in millisecond time domain for ZnS:Mn phosphors. At liquid nitrogen temperature the life time values are in the range of 0.08 to 42.86 microsecond in case of CaS, and 0.65 to 13.87 microsecond in case of ZnS.

In 1996, Park et al. [20] had studied time-resolved luminescence data from heavily nitrogen doped ZnSe. The luminescence exhibited a decay time and a rise time, which increased with decreasing energy of observation. Furthermore, both the decay times and rise times decreased with increasing temperature. These observations are consistent with the following model: (i) a band of states was created due to fluctuations in the ionized impurity concentrations; (ii) a portion of the carriers captured by the shallower impurity states were transferred to deeper states prior to recombination. In 2000, Suyver et al.[21] had studied the luminescence properties of nanocrystalline ZnSe:

Mn^{2+} prepared via an inorganic chemical synthesis. Photoluminescence spectra showed distinct ZnSe and Mn^{2+}` related emissions, both of which were excited via the ZnSe host lattice. The Mn^{2+} emission wavelength and the associated luminescence decay time depend on the concentration of Mn^{2+} incorporated in the ZnSe lattice. Temperature-dependent photoluminescence spectra and photoluminescence lifetime measurements were also presented and the results were compared with those of Mn^{2+} in bulk ZnSe. Better results are expected for ZnSe which has a valence band-edge at higher energy with respect to ZnS. In 2003, Thaddeus et al [22] had synthesized Cu(II) doped ZnSe nanoparticles using molecular cluster precursors. The Cu(II) dopant had the effect of quenching the ZnSe band edge emission, yet only weak emission from Cu(II) centers was observed. An X-ray Absorption Fine Structure (XAFS) experiment was performed on the Cu(II) doped ZnSe nanoparticles. In 2005, Changlong et.al [23] had studied ZnSe hollow spheres synthesized hydrothermally at 140 °C, by using reducing agent. Both the transverse optic (TO) and longitudinal optics (LO) phonon peaks in the Raman Spectra of the ZnSe showed the obvious shift to lower frequency compared to bulk values, a blue shift has been observed in PL spectra. In 2006, Shan et at [24] had prepared Wurtzite ZnSe nanowires on GaAs substrates by a metal-organic chemical vapour deposition system. Electron microscopy showed that they were smooth and uniform in size. Both transmission electron microscopy and x-ray diffraction reveal the wurtzite structure of the nanowires, which grows along the (0001) direction. Raman scattering studies on individual nanowires were performed in the back-scattering geometry at room temperature. Besides the commonly observed longitudinal and transverse optical phonon modes, a possible surface mode located at 233 cm^{-1} is also observed in the Raman spectrum. A peak located at 2.841 eV was clearly observed in the photoluminescence spectra of the nanowires, which can be assigned to near band edge emissions of wurtzite ZnSe. In the same year, Venkatachalam et al. [25] deposited Zinc selenide (ZnSe) thin films onto well cleaned silicon (100) and glass substrates at different substrate temperatures (483–589 K) using vacuum evaporation method under a vacuum of 4×10^{-3} Pa. The compositions of the deposited films were determined by Rutherford backscattering spectrometry and the percentage of iodine concentration is calculated as (ZnSe) I 0.001. The x-ray diffractograms reveal the cubic structure of the film oriented

along the (111) direction. In optical studies, the transition of the deposited film is found to be a direct allowed transition. The optical energy gaps of the deposited films are found to be in the range from 2.72 to 2.60 eV. ZnSe/silicon Schottky diodes were fabricated. From the current–voltage measurement, the ideality factor was found to be in the range 2.01–3.51. From the capacitance–voltage studies, the built in potential was found to be 1.51 V. The values of effective carrier concentration (NA) and the barrier height are calculated as 4.37×10^{11} cm^{-3} and 1.95 eV, respectively.

CHAPTER 2

PREPARATION AND CHARACTERIZATION OF NANOPHOSPHORS

2.1 Methods of Preparation

During the last one decade, a number of synthesis methods have been reported for the preparation of various intrinsic semiconductor nanocrystals and the method of preparation for doped nanoparticles are still evolving. Generally the doping of bulk semiconductors is carried out by high temperature thermal diffusion or molecular deposition techniques including chemical vapor deposition, atomic layer epitaxy, gas phase deposition, vacuum evaporation, etc. in the case of nanoparticles, the incorporation of impurities into quantum-confined systems, containing only few tens of atoms or molecules is much more difficult and complex because no conventional high temperature processes can be applied. In this case, doping has to be carried out by low temperature processes, mostly by wet-chemical synthetic routes. The doping through wet-chemistry invites some new difficulties that are not encountered in the case of bulk material. For example, the dopant ions used in the reaction may preferably precipitate, as a stable phase, prior to the incorporation into the host lattice leading to very low or no doping at all. Further, even though dopant ions are incorporated into the lattice, these may tend to diffuse on to the nanoparticles surface or the surrounding matrix because the impurity ions are always only a few lattice constant away from the surface. Thus the preparation of effectively doped semiconductor nanocrystals and their application in the nanotechnology frontier still remain a challenging task.

2.1.1 Synthesis of doped nanophosphors

There are two general approaches for the synthesis of nanomaterials; a) top-down and b) bottom-up techniques. The top-down technique , it starts with a large scale object and gradually reduces its dimensions it covers mostly physical methods such as e-beam lithography , which shines radiation through a templates on to a surface coated with a radiation sensitive resist , atomic force manipulation , gas-phase condensation , aerosol spray etc; whereas the bottom up approach , where individual atom or molecule are placed or are self assembled precisely at the required places ,basically include all wet-chemical methods like , reverse-micelle , sol gel synthesis, colloidal precipitation for the synthesis of luminescent nanoparticles , the bottom–up approach is generally preferred .

before discussing the process adopted in the present investigation , a brief review of some of the known methods of synthesis are discussed in the following sections.

2.1.2 General bottom up methods

Organ metallic reaction route, is reported for the synthesis of ZnSe:Mn^{2+}, ZnS:Mn^{2+},CdSe:Mn^{2+}etc. In this technique, the nanoparticles preparation and its doping are carried out by the co-precipitation reaction of organometallic-reagent at relatively high temperature (~300 ^{o}C) under controlled environmental conditions. This route has the advantages of making nanoparticles with better crystallites; however, the laborious process, high cost , rare availability and often toxic nature of the reagent, etc, make this method largely non adaptive. Another well known process of nanoparticle synthesis is the reverse-micelle routes. During this process the particles are precipitated within a size restricted water pool of the water-in-oil ternary micelle system. The size of water pool is controlled by the concentration ratio W=[H_2O]/[AOT]. This method has been widely used for the synthesis of monodispersed nanoparticles of CdS, Cd_{1-x} Mn_xS, etc. In the case of doped nanoparticles; this method has some difficulties due to the unavoidable use of high concentration of the surfactant medium, which hinders the doping as well as particle separation process. The sol gel synthesis is another method used for making nanophosphors.

2.1.3 Synthesis of ZnSe nanophosphors

Nanophosphors will prepared by aqueous colloidal precipitation method at room temperature. The colloidal precipitation technique has been found to have a number of advantages including easy process ability at ambient conditions , possibility of doping of different kinds of impurities with high doping concentration even at room temperature, good control over the chemistry of co-doping particularly when different impurities are in-corporated simultaneously in the host lattice, easiness of surface capping with a variety of different steps involved in the synthesis process of nanophosphors .

2.1.4 Preparation of doped ZnSe nanocrystals

Different synthesis methods viz. reverse micelles, homogeneous precipitation and colloidal precipitation, etc. have been carried out by various researchers to prepare the doped nanocrystalline ZnSe phosphors [20-25]. By comparing properties of the materials obtained from different routes, colloidal precipitation was found better for producing efficiently luminescent nanophosphors in terms of process simplicity, effectiveness of doping and higher yield etc. Different analytical grade chemicals have been purchased from sd-fine Chemicals, India. The synthesis employed co-precipitaton reaction of inorganic precursors of Zn^{2+} and Se^{2-} with dopant ions (Mn^{2+}, $Cu^{2+}$and Co^{2+}) in aqueous medium containing the capping molecules of 1% PVP prepared by dissolving 1gm of PVP in 100ml of distilled water. The different concentrations of impurities in solution were maintained at (10%, 5%, 1% & 0.1%) with Zn^{2+}, for ZnSe:Mn, ZnSe:Cu, ZnSe:Co samples. 2.195 g of $C_4H_6O_4Zn.2H_2O$ has been dissolved in 50 ml of distilled water to obtain 0.2 M solution. 1.7294 g of Na_2SeO_3 has been dissolved in 50 ml of distilled water to get 0.2 M of solution. In the synthesis of ZnSe, 25ml of $C_4H_6O_4Zn.2H_2O$ solution was mixed with solution of polyvinylpyrrolidone(PVP), the capping agent was added to avoid agglomeration of grown nanoparticles. Nanoparticles with polymer capping were precipitated by slowly adding 25 ml of 0.2 M Na_2SeO_3 solution to the above mixture. A white colloidal suspension was obtained immediately after adding Na_2SeO_3 solution. The precipitates were separated by 2000 rpm centrifugal machine and washed several times with distilled water. Then the sample was dried in a vacuum oven at a temperature of about 80 ^oC.

2.2 Characterization Techniques

2.2.1 X-ray diffraction studies (XRD)

X-ray diffraction is the most wide spread technique for determining the phase identification, crystal structure, lattice parameter of the crystalline solids. A typical powder XRD instrumentation consist of four main components such as X-ray source, specimen stage, receiving optics and X-ray detector as shown in fig.3. The source and detector with its associated optics lie on the circumference of focusing circle and the sample stage at the center of the circle. The angle between the plane of the specimen and

the X-ray source is θ, known as Braggs angle and the angle between the projection of X-ray and the detector is 2θ.

For the XRD analysis, fine powder samples were mounted on the sample holder and the powder was assumed to consist of randomly oriented crystallites. When a beam of X-ray is incident on the sample, X-rays are scattered by each atom in the sample. If the scattered beams are in phase, these interfere constructively and one gets the intensity maximum at that particular angle. The atomic planes from where the X-rays are scattered are referred to as 'reflecting planes

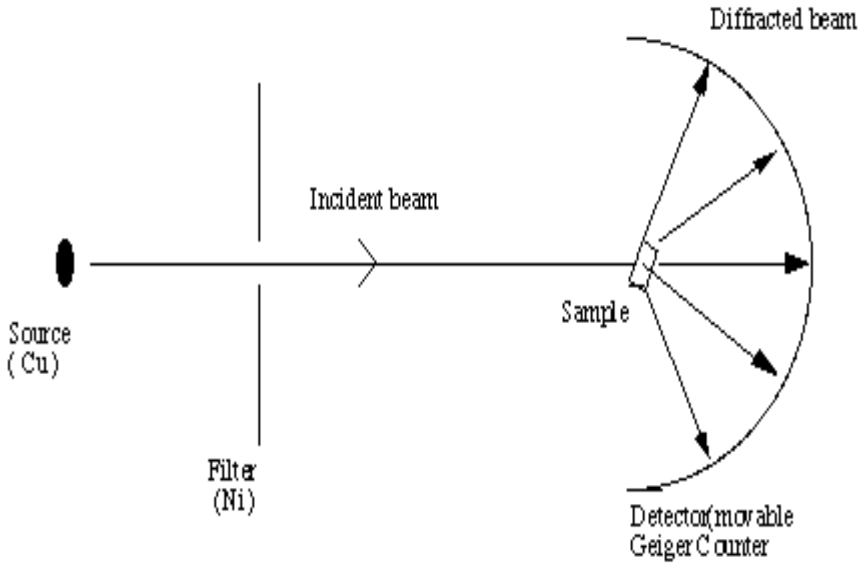

Fig.3-X-ray diffraction (XRD)

The Bragg's law relates the wavelength (λ) of the X-ray reflected, the spacing between the atomic planes (d) and the angle of diffraction (θ) as follows:

$$2d \sin \theta = n \lambda$$

For the first order diffraction, n=1, and knowing θ and λ , one can calculate the interplanar spacing d–value for a particular plane. After recording the X-ray diffraction pattern, first step involves the indexing of XRD peaks. The indexing means assigning the

correct Miller indices to each peak of the diffraction pattern. The correct indexing is done only when all the peaks in the diffraction pattern are accounted for the process. There are three main methods for indexing a diffraction pattern, (i) comparing the measured XRD pattern with the standard data base (JCPDS-cards) (ii) analytical methods (iii) graphical methods.

In case of fine particles, with reduction in the size of the particles, the XRD lines get broadened, which indicates clearly that particle size has been reduced. The line broadening can be a measure of the average size of the crystallites by using the Scherrer equation:

$$Dv = K\lambda/\beta \cos\theta$$

where; Dv is the average particle size
K is the Scherrer constant
λ is wave length of the radiation
β is the integral breadth of the peak located at angle θ.

2.2.2 Transmission electron microscope

Transmission electron microscopy (TEM) is used to obtain information from samples that are thin enough to transmit electron. In TEM, the whole area of observation is illuminated using an electron source of adequate intensity. The transmitted electrons are generally used to form either an image or a diffraction pattern of the specimen .The formation of image and electron diffraction in TEM can be understood from schematic ray diagram as shown in fig.4.

When a crystal of lattice spacing 'd' is illuminated with electrons of wavelength 'λ', the diffracted waves will be produced at specific angles 2θ for n =1, satisfying the Bragg's condition

$$2d \sin\theta = \lambda$$

The diffracted waves form diffraction spots on the back focal plane. In an electron microscope, the use of electron lenses allows the regular arrangement of diffraction spots to be projected on a screen and the electron diffraction pattern can be observed. If the transmitted and the diffracted beam interfere on the image plane, a magnified image can be observed. The space where the diffraction pattern forms is called the reciprocal space, while the space at the image plane or at a specimen is called the real space.

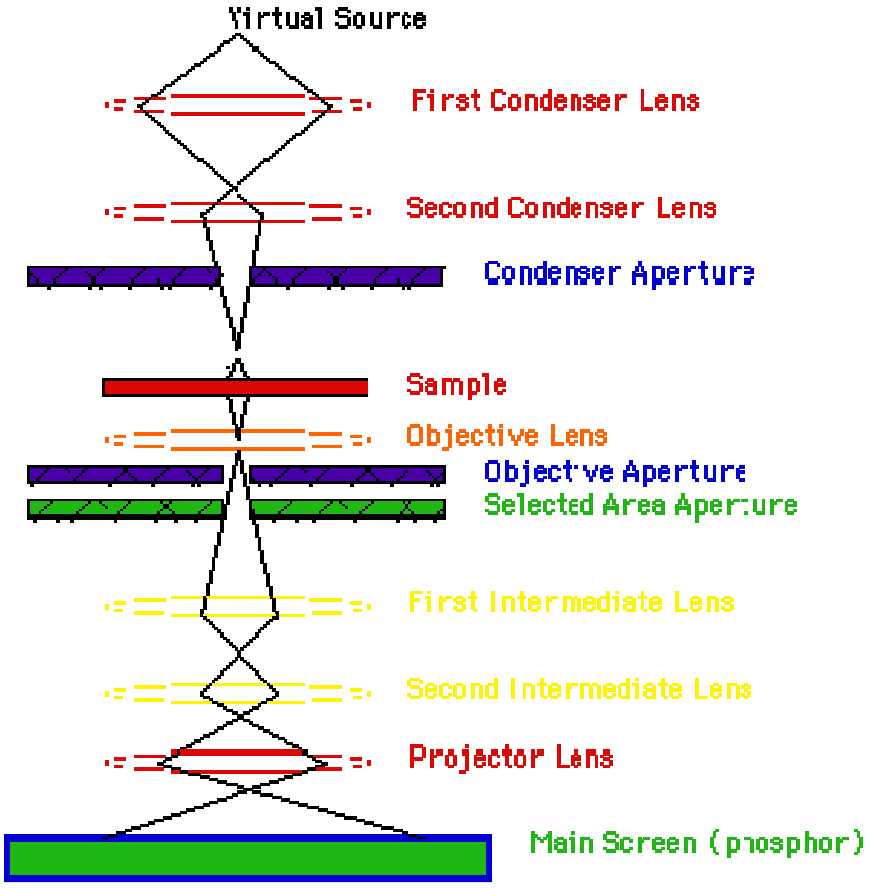

Fig.4-Transmission electron microscope

In TEM, by adjusting the electron lenses, both the microscope images and diffraction patterns can be observed. Thus in the analysis of microstructures of materials, both observation modes can be successfully combined. In an investigation of electron diffraction pattern, the electron microscope images of the nanophosphor is first observed of the whole area and then by inserting an aperture in a specific area and adjusting the

electron lenses a diffraction pattern of the area is obtained. The latter observation mode is called selected area electron diffraction (SAED). Because a selected area diffraction pattern can be obtained from each grain, the crystal structure and mutual crystal orientation relationship between adjacent grains can easily be clarified. The observational dimension selected from the object is usually limited to about 0.1 micrometer in diameter. However, in micro diffraction method, the diffraction pattern can be obtained from an area correspondingly to only a few nanometers in diameter. Then, by passing the transmitted beam or one of the diffracted beams through an aperture and changing to the imaging mode, the image with enhanced contrast can be observed. The observation mode using the transmitted beam is called the bright field method, and the image observed is a bright field image. When one of the diffracted beams is selected the observation mode is called as dark field method, and the image observed is a dark field image.

2.2.3 Experimental Set-up for Pulse-Excitation Method

The experimental set-up employed to record the short-lived phosphorescence in the micro-seconds time domain is shown in Fig.6.

It consists of the following parts:

1. Nitrogen laser as the excitation source
2. Sample held at an angle of 45° to the incident radiation
3. Glass slab to filter out UV scattered light, if any.
4. Monochromator as a wavelength selective element
5. Photomultiplier tube with power supply as a phosphorescence detective element
6. Data analyser as a PC and a digital storage oscilloscope

For room temperature (300 K) studies, the sample is taken in the form of a pellet or in powder form in a groove specially prepared in a perspex sheet or in the form of a thin film pasted with xylene on a glass plate. For liquid nitrogen temperature studies, a specially designed cryostat is used. Nitrogen laser is the most suitable excitation source (337.1 nm) to irradiate the doped phosphors as laser energy excites the luminescent

centers introduced by the dopants in the phosphors very effectively. High photon flux density (10^{19} photons per pulse) of the laser is very useful to excite the short-lived shallow trapping states which otherwise were impossible to excite using conventional light sources like mercury vapor lamp or xenon flash lamp.

Fig.5-Photograph of experimental set-up for life-time measurement studies at room temperature.

Short pulse-width of Nitrogen laser (10 ns) is helpful to determine the lifetime values accurately in the milli- and micro-seconds time domain without introducing its own effect. The short lived phosphorescence from the sample at an angle of 90° to the incident beam was collected by a fast photomultiplier tube through an assembly of monochromator as a wavelength selective element and glass slab to filter out the UV radiation. The hyperbolic decay signals from the phosphors are recorded by a fast digital type storage oscilloscope, which is interfaced with a computer. Computer simulations are

done to calculate lifetime values accurately of the different excited states contributing to the phosphorescence hyperbolic decay.

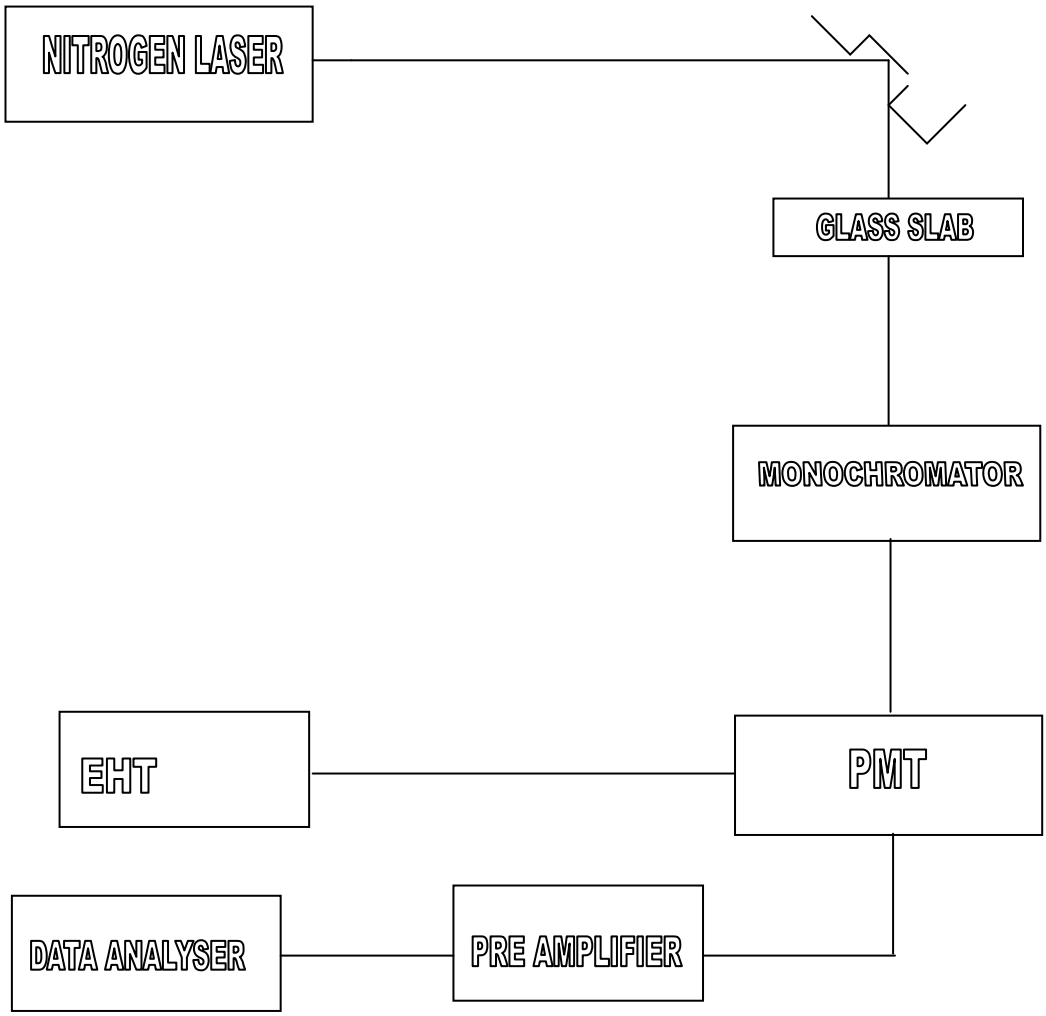

Fig.6-Block diagram of experimental set-up for life-time measurement

The functions and working of various components used in this experimental set-up are discussed as below:

2.2.3.1 Nitrogen Laser

When a high current transverse electrical discharge passes through the nitrogen gas that is flowing at a relatively low pressure(30-50 torr), it can generate a pulse of coherent radiation at the wavelength of 337.1nm. The wavelength lies in the ultraviolet region of the electromagnetic spectrum. The laser action begins when a molecule of nitrogen absorbs energy by colliding with an electron that moves in the plasma column. This encounter leaves the molecule in the excited state from where it usually falls into a state of lower energy by emitting a photon of wavelength 337.1nm. The emitted photon may encounter another molecule of nitrogen in the excited state and stimulate it to emit an identical photon. In this way the two emitted photons proceed in the same direction, with their waves in lockstep. The resulting pulsed radiation contains twice the energy of each photon and the emitted photons are in phase with each other. This process is called the laser action. The laser action will continue as long as the growing pulse encounters more excited molecules of nitrogen along its path than it does absorbing molecules. But the laser action soon stops due to the short lifetime of the upper excited laser level.

The important properties of nitrogen laser that are useful to conduct the phosphorescence decay measurement are summarized as follows:

1 The output wavelength = 337.1 nm (ultraviolet region) so electronic energy levels of phosphors can be easily excited with this UV radiation as this energy matches very much with the bandgap energies of phosphors under study.
2 Pulse-width = 5-10 ns which is very small and lifetime values of the order of microseconds can be easily measured, without taking into account the pulse-width of the exciting nitrogen laser source.
3 High peak power ~ kW can easily excite shallow trapping states, which were earlier difficult to excite with ordinary UV light sources.
4 High repetition rate (10 to 100Hz), which can be changed by adjusting the power supply components to get the fast data collection rate for decay measurements.

All these characteristics of Nitrogen laser are due to the typical energy levels of nitrogen molecule which are discussed in detail as under: The potential energy level diagram of N_2 molecule relevant to important laser transitions is shown in fig.7. Important laser transitions are $C^3\pi_u \rightarrow B^3\pi_u$, which is the second positive system (ultraviolet region) and $B^3\pi_g \rightarrow A^3\Sigma^+_u$ called first positive system (IR region) .

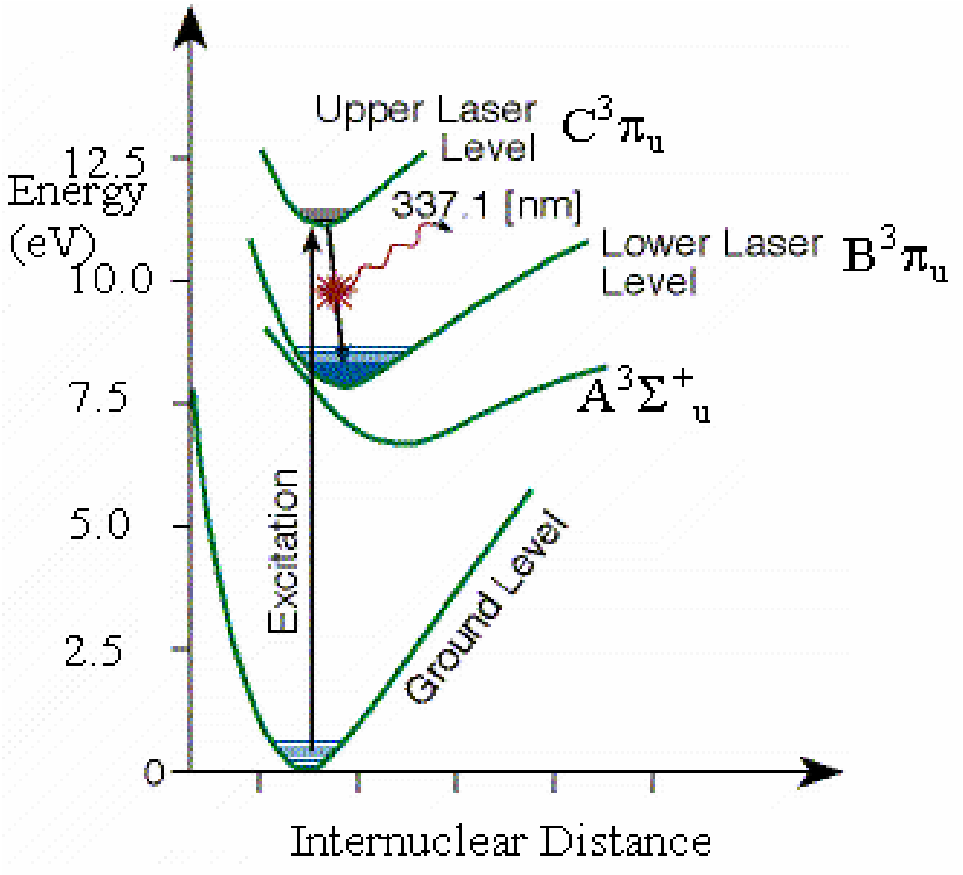

Fig.7-Energy level diagram of nitrogen molecule

In the second positive system, following vibrational transitions are observed:

0 – 0: 337.1nm 0 – 1: 357.7nm

0 – 2: 380.5nm 1 – 0: 315.9nm

Out of these (0 - 0) transition is the most prominent and easily obtainable in electrical discharge of nitrogen gas in this laser. In the first positive system various bands

from 735 to 1235nm have been observed. The radiative lifetimes of different states at low pressure are:

C ~ 40 nsec. ; B ~ 5.8 μsec. ; A ~ 1.2 sec

These lifetimes are actually pressure dependent .On increasing the pressure the rate of collisions increases and lifetime of C level decreases. At atmospheric pressure the pulses of the order of picoseconds can be obtained in the second positive system.

The lifetimes of C and B levels make continuous wave (CW) laser between these levels which is impossible; since for a continuous laser one generally requires a metastable upper level and fast decaying lower level. In nitrogen laser, in both positive systems, lifetime of upper level is much shorter than the lower level. Therefore both are inherently transient laser systems and can be operated by pumping upper level faster than the lower level.

Under certain approximations population inversion exists only for a time:

$$t < \frac{1}{Y_{21} + \tau_{21}} \qquad (2.5)$$

where; Y_{21} – collisional de excitation rate from level C to B

and τ_{21} – radiative lifetime for the transition C $\rightarrow$ B

Thus if we neglect Y_{21}, population inversion can exist only for a time of ~ 40nsec. For an electron density $N_e \sim 10^{14}$ cm^{-3}, $Y_{21} \sim \tau^{-1}{}_{21}$ and inversion duration is further reduced. Also the above calculation neglects loss due to stimulated emission. Hence in actual case, population inversion lasts only for a time 10-20 ns (17-20). One advantage of short upper state lifetime is that gain for the transition is quite high. In fact nitrogen laser generally operates in a super-radiant mode i.e. without feed-back. Spontaneous emission

gets amplified along the direction of laser axis. High power pulse can be built up even in a single pass.

A convenient way of producing population inversion is via an intense electrical discharge of N_2 gas. The discharge must be rapid enough so that maximum energy in the gas is deposited in a time of 10-20 ns; energy spent afterwards is a waste because inversion ceases to exist. Electrons produced in the discharge undergo inelastic scattering with N_2 molecules creating excitation and ionization. From the potential energy diagram shown in Fig.8, it is seen that the minimum of the potential energy for the C state lies directly above that for the ground state, while the minimum for B state lies at greater inter-nuclear separation. Hence the cross section for the excitation of v = 0 level for C state is greater than the cross section for the excitation of v = 0 level of B state. In case of $N_{2\ gas}$, since ground state is singlet while B and C are triplet states, a transition is possible only through electron exchange. Electrons with energy in the range 12-18 eV will predominantly excite C level. At energy of 16 eV the ratio of cross sections is maximum.

2.2.3.2 Monochromator

This is an instrument that provides a calibrated source of nearly monochromatic light at various wavelengths of interest. Such a device is called a *monochromator*, the name being derived from the two words "mono" meaning one and "chroma" meaning color. In short, a monochromator is a device that selects light in a narrow band of wavelengths from a beam of light in which a range of wavelengths are present.

In our case constant deviation spectrometer is used as a monochromator. It consists of a constant deviation prism shown in fig.8 .

In this prism the emergent ray is always perpendicular to the incident ray. This prism is placed on a prism table of a monochromator, which can be rotated about a vertical axis by means of a calibrated rotating drum. Firstly the spectrometer is calibrated by exposing it to mercury vapor lamp. The prism is then adjusted corresponding to the green light (546nm). Then mercury lamp is removed and the sample is to placed in

front of slit in a perspex slab having groove at 45° to both monochromator and nitrogen laser. The drum of the monochromator is adjusted at the maximum intensity of the broad emission spectrum of the phosphor

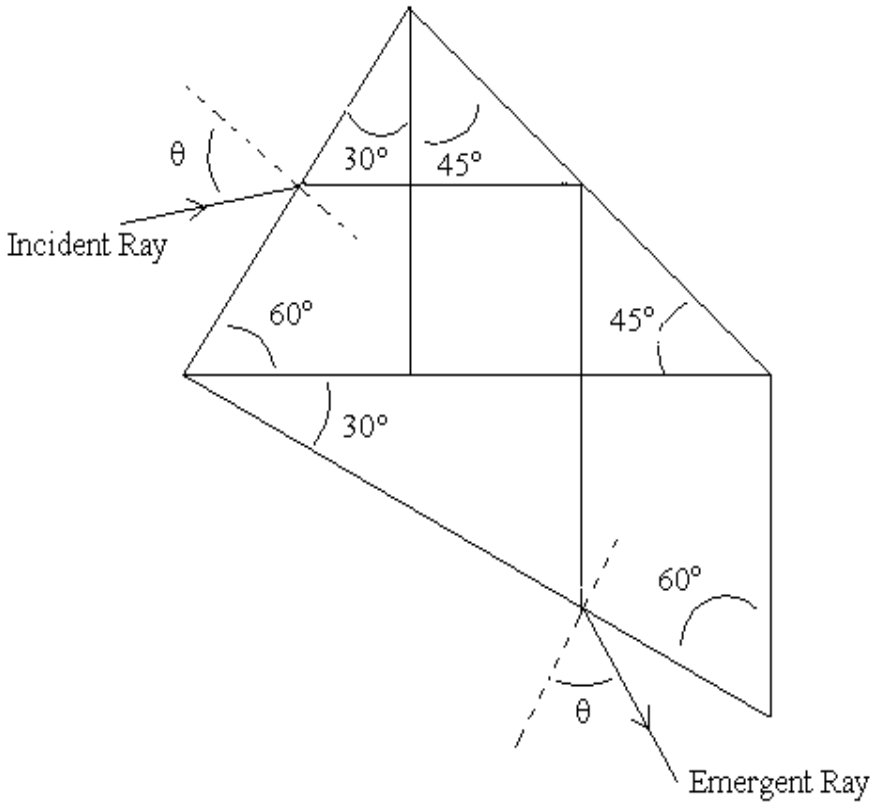

Fig.8-Constant deviation prism used in monochromator

2.2.3.3 Photomultiplier Tube:

The photomultiplier tube (PMT) fig.9 detects the phosphorescence signal output from the monochromator and converts it to an electrical signal that can be read by the fast digital storage type oscilloscope. When photons exit the monochromator, they pass into the PMT and hit a photocathode. When the photon hit the photocathode, it emits secondary electrons due to the photoelectric effect. These electrons are accelerated in a vacuum across a series of dynodes, which are held at increasingly more positive voltages.

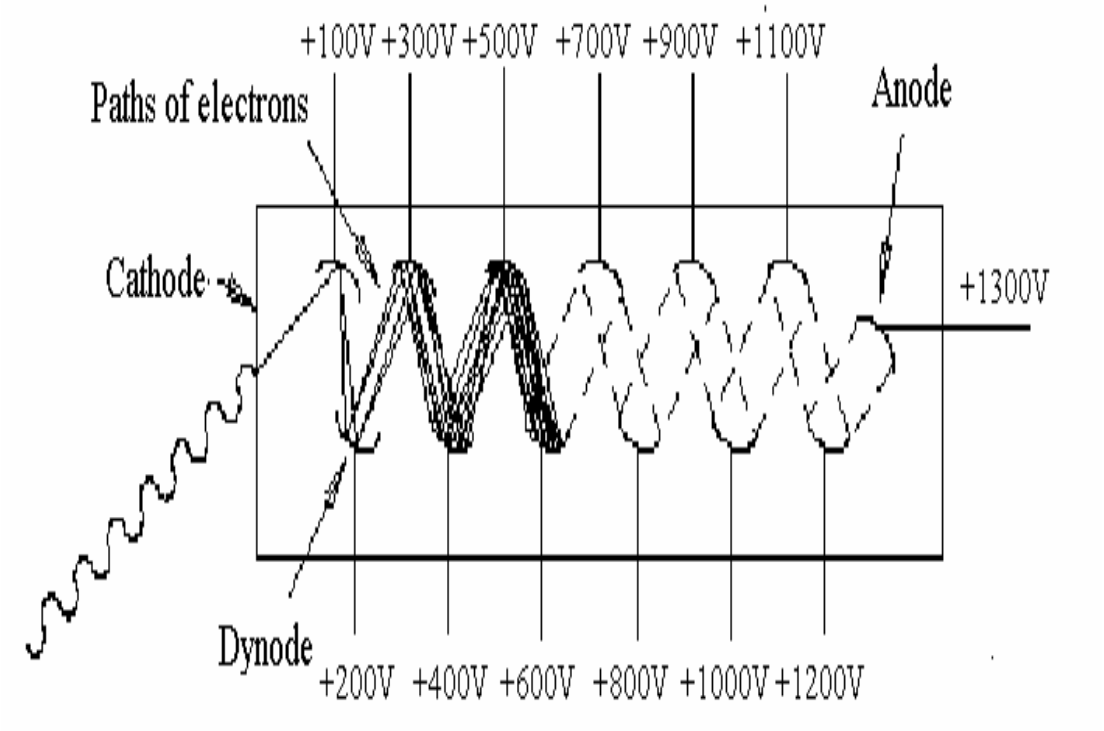

Fig.9-Basic diagram of PMT tube

Secondary electrons are produced each time an electron encounters a dynode. There is generally a factor of 4 multiplications for each electron (one electron hitting the dynode equals four electrons emitted). This effect generates 4^N (N is the number of dynodes) electrons for each photoelectron emitted. The electrons are collected at the anode where these are detected and produce a current output in the form of a negative pulse. In present case RCA 8053 photomuliplier tube is used. The signal after proper amplification is fed to a digital storage type oscilloscope, which is interfaced with a fast computer for further analysis of three lifetime components.

CHAPTER 3

RESULTS AND DISCUSSION

3.1 Theory of Phosphorescence

When samples are exposed to the laser radiation, the electrons are raised from valence band to the excited states, then these electrons may return to the valence band with the emission of characteristic luminescent radiation. If n be the number of electrons in an excited state at time, t, and, dn, be the number of electrons decaying in time, dt, then for this decay:

$$\frac{dn}{dt} = -pn \tag{3.1}$$

or

$$\frac{dn}{n} = -pdt \tag{3.2}$$

which on integration gives:

$$n = n_0 e^{-pt} \tag{3.3}$$

or intensity is given by

$$I = I_o e^{-pt} \tag{3.4}$$

where I is the intensity of phosphorescence radiation at time, t, and Io, the intensity of radiation at cut-off position and the constant, p, is the transition probability of the corresponding radiative transition. A plot of ln (I) vs time will be a straight line in case of single set of traps of energy, E. From slope of line we can calculate value of trap-depth, E, according to the Boltzmann's equation

$$p = S e^{-E/kT} \tag{3.5}$$

where S is escape frequency factor $\left(\sim 10^9\ s^{-1}\right)$ or attempt to escape frequency [26-27] and may be interpreted as the number of times per second that the thermal quanta from crystal vibrations try to eject the electron from the trap, multiplied by the probability of a transition from the trap to the conduction band, k is the Boltzmann's constant and T, the absolute temperature. However, in most of the cases, when we come

across the interaction of radiation with solids, there are trapping levels at many different depths. In an ideal case of uniform distribution, one can assume an equal number of traps at all depths. Under this assumption if n_E be the number of traps in the energy range, E, and, E+dE, the intensity of phosphorescence at any time t is given by:

$$I = \int n_E S e^{-E/kT} \exp\left(-S t e^{-E/kT}\right) dE \tag{3.6}$$

which on integration yields:

$$I = n k T \left(1 - e^{-St}\right)/t \tag{3.7}$$

$$I = n k T t^{-1} \quad \text{when St} >> 1 \tag{3.8}$$

However in most of the cases, the distribution of traps, at different depths may not be uniform and distribution of the traps can be studied from the equation

$$I = I_0 t^{-b} \tag{3.9}$$

where, b, is called the decay constant. Such types of decay curves due to superposition of number of exponential decays are popularly known as hyperbolic decay curves. If the value of, b, is unity, one can say that the distribution of traps is uniform, otherwise, it is said to be non-uniform. In the present case, a plot of ln (I) vs. time does not show linear relationship because of the superposition of the number of exponential decays. The different components of a decay curve may be considered as emission due to traps of different depths. Thus it is reasonable to assume as the number of exponentials increase, the decay curve changes from a exponential to a hyperbolic decays. The minimum number of exponentials required is three to form a hyperbolic decay curve. The decay curves can be peeled-off into three components by the peeling off method of Bube [28-30]. The results of decay curves can be expresses as:

$$I = I_{01} \exp(-p_1 t) + I_{02} \exp(-p_2 t) + I_{03} \exp(-p_3 t) \tag{3.10}$$

where p_1, p_2 and p_3 are the transition probabilities.

3.1.1. Photoluminescence studies of pure and doped ZnSe nanophosphors

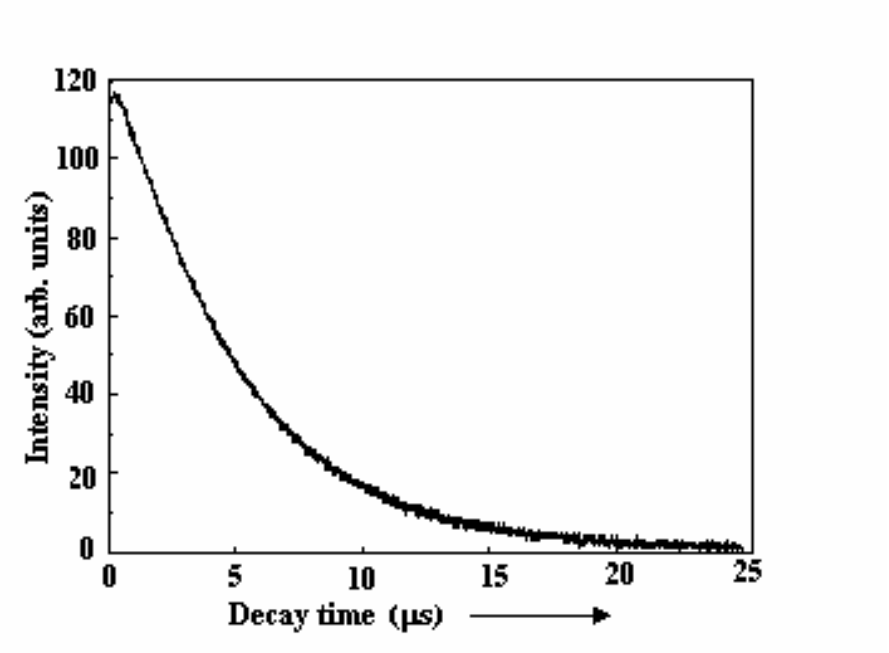

Fig.10-Hyperbolic type of phosphorescence decay curve for ZnSe:Mn (10%)

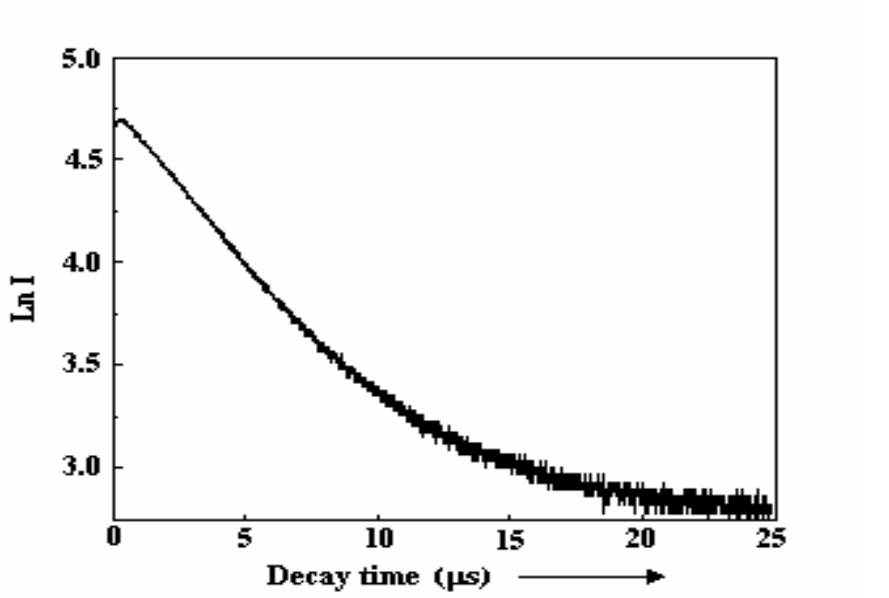

Fig.11-ln I vs decay time graph for ZnSe:Mn (10%)

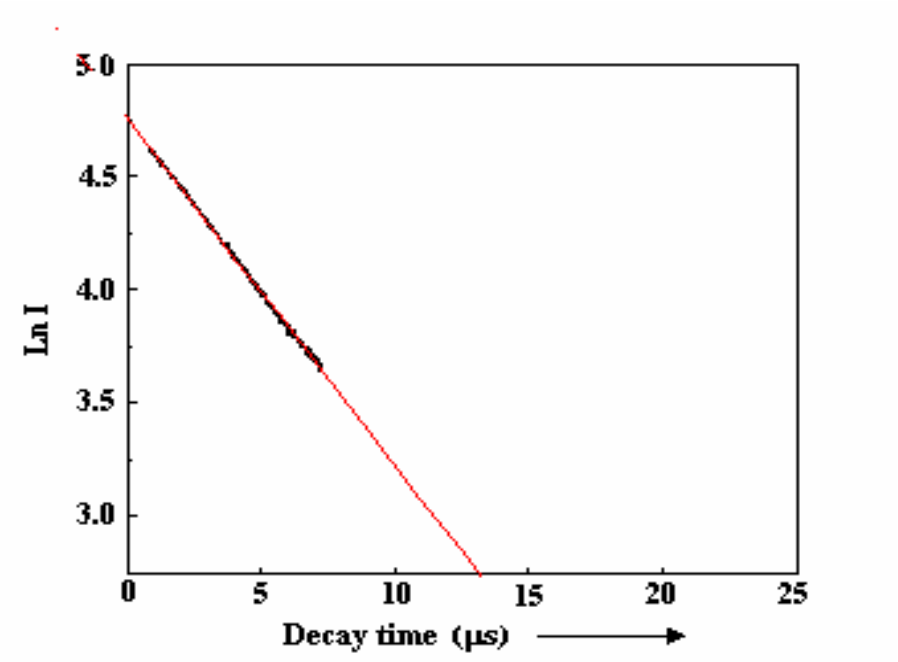

Fig.12.a.-ln I vs decay time graph for ZnSe:Mn (10%) which yields slope of curve; $p`=146627\ s^{-1}$, $\tau`=6.82\ \mu s$, $E`=0.228$ eV.

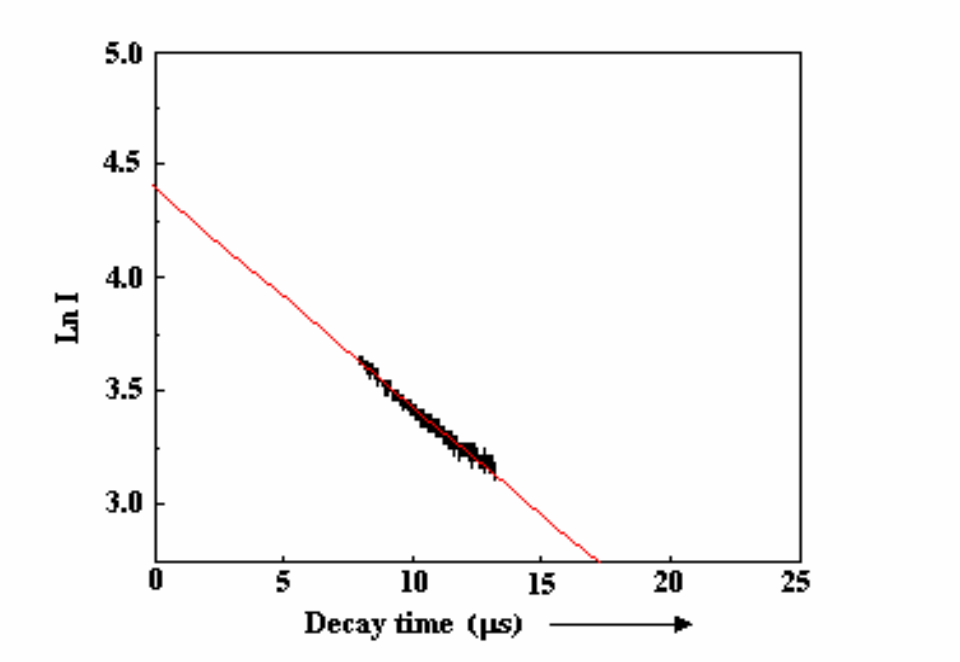

Fig.12.b.-ln I vs decay time graph for ZnSe:Mn (10%) which yields slope of curve; $p``=76923.07\ s^{-1}$, $\tau``=13.0\mu s$, $E``=0.245$ eV.

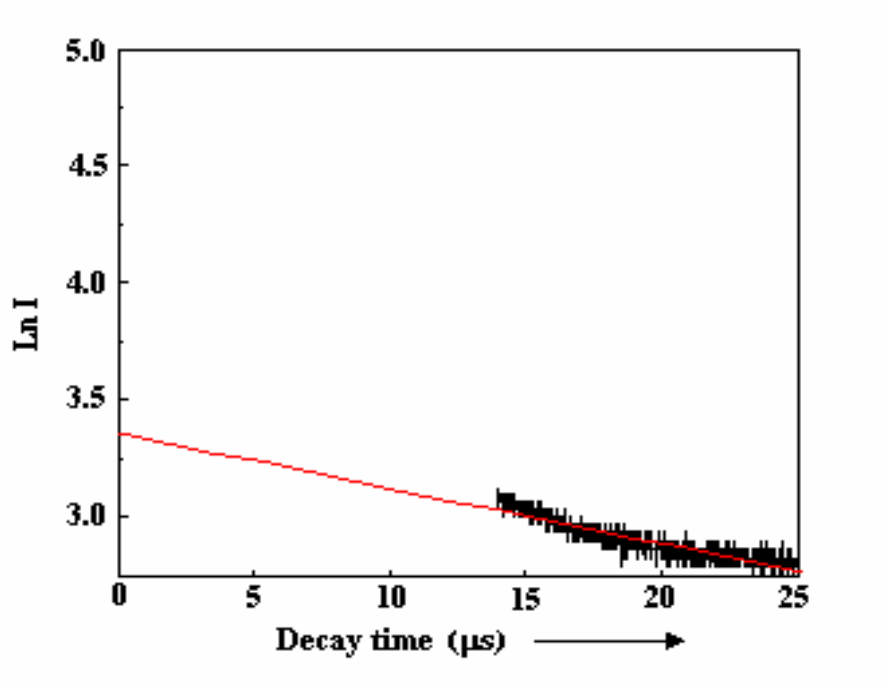

Fig.12.c.-ln I vs decay time graph for ZnSe:Mn (10%) which yields slope of curve; $p^{```}$=22222.22 s^{-1}, $\tau^{```}$=45.0μs, $E^{```}$=0.271eV.

Table 3.1:- Excited state lifetime values of pure and doped ZnSe nanophosphors recorded at room temperature

S.No	Phosphor: impurity(wt%)	Wavelength (nm)	Lifetime values(μs)at 300K		
			τ`	τ``	τ```
1	ZnSe	409	6.22	12.9	50.25
2	ZnSe:Mn(10%)	422	6.82	13.0	45.0
	ZnSe:Mn(5.0%)	422	7.00	17.3	243.3
	ZnSe:Mn(1.0%)	407	6.54	11.1	28.8
	ZnSe:Mn(0.1%)	443	6.72	16.1	297.0
3	ZnSe:Cu(10%)	440	12.4	28.7	145.0
	ZnSe:Cu(5.0%)	475	4.9	5.9	10.4
	ZnSe:Cu(1.0%)	440	7.48	17.4	67.8
	ZnSe:Cu(0.1%)	420	7.36	14.6	59.2
4	ZnSe:Co(10%)	449	6.99	11.9	46.7
	ZnSe:Co(5.0%)	427	7.01	13.5	51.7
	ZnSe:Co(1.0%)	475	6.98	13.6	53.1
	ZnSe:Co(0.1%)	456	6.44	10.2	38.3

Table 3.2:- Trap-depth values of pure and doped ZnSe nanophosphors recorded at room temperature

S.No	Phosphor: impurity(wt%)	Wavelength(nm)	Trap depth values (eV)		
			E`	E``	E```
1	ZnSe	409	0.226	0.245	0.280
2	ZnSe:Mn(10%)	422	0.228	0.245	0.271
	ZnSe:Mn(5.0%)	422	0.229	0.253	0.321
	ZnSe:Mn(1.0%)	407	0.227	0.241	0.266
	ZnSe:Mn(0.1%)	443	0.228	0.251	0.326
3	ZnSe:Cu(10%)	440	0.244	0.266	0.308
	ZnSe:Cu(5.0%)	475	0.220	0.225	0.239
	ZnSe:Cu(1.0%)	440	0.231	0.253	0.288
	ZnSe:Cu(0.1%)	420	0.230	0.248	0.284
4	ZnSe:Co(10%)	449	0.225	0.243	0.278
	ZnSe:Co(5.0%)	427	0.229	0.246	0.281
	ZnSe:Co(1.0%)	475	0.229	0.246	0.282
	ZnSe:Co(0.1%)	456	0.222	0.239	0.273

Hyperbolic decay curves have been observed in case of pure and doped ZnSe nanophosphors with variable concentration of Mn, Cu and Co impurities. Pure exponential components of decay curves were extracted from the hyperbolic decays (Fig. 11) with the help of computer software as shown in Fig (12a-c). The excited state life-times in case of pure and doped ZnSe nanophosphors are in microseconds time domain and varying from 6.22μs to 50.25μs for pure ZnSe (Table 3.1) and the excited state lifetimes in case of doped ZnSe nanophosphors vary from 4.4μs [ZnSe:Cu(5%)] to 297.00μs [ZnSe:Mn(0.1%)] (Tables 3.1) at room temperature. The lifetime values don't show any appreciable trend with variation of impurity concentration as shown in (Table 3.1) and the emission wavelength also don't show much change with addition of impurity as blue emission is observed for all the samples. The trapping states which contribute significantly to the luminescence range from 0.226 to 0.280 eV in case of pure ZnSe nanophosphors (Table 3.2.). When Mn, Cu, and Co impurities are added to ZnSe nanophosphors, the trap depth values lie between 0.220eV [ZnSe:Cu(5%)] to 0.326eV [ZnSe:Mn(0.1%)] as shown in (Table3.2). However the decay curves remain hyperbolic in nature and which does not change with the addition of the impurities.

In the present investigation, the lifetime values are in microsecond time regime. This suggests that emission is due to the weak magnetic dipole transitions. But the excited state lifetimes and trap-depth values do not show appreciable trend with variation in impurity concentration, these decrease and increase randomly. Moreover blue emission is observed for all the samples with slight change in emission wavelength with impurity concentration. So it is clear from the above observation that Mn, Cu and Co dopants in ZnSe nanoparticles do not give their characteristic emission; these impurities are just perturbing the levels of the host. Although dopant characteristic emission is not observed, however the decay time and emission wavelength has been monitored (Table 3.1).

3.2 Morphological Characterization

3.2.1 X-ray diffraction studies

X-ray diffraction (XRD) is an efficient tool for the structural analyses and morphological characterization of crystalline materials. In the present studies, XRD

patterns have been recorded using D/max Rint 2000 Rigaku (Tokyo) powder X-ray diffractometer using copper characteristic wavelength of 1.5418 $\overset{o}{A}$ operated at 40kV and 40mA keeping step size (0.02) degree s^{-1}. Peak broadening has been observed in recorded diffraction patterns, which shows the formation of nanocrystallites. Fig. 13 shows the XRD pattern recorded for pure ZnSe. Comparison of the recorded XRD pattern with standard JCPDS data file 10979 confirms the wurtzite structure.

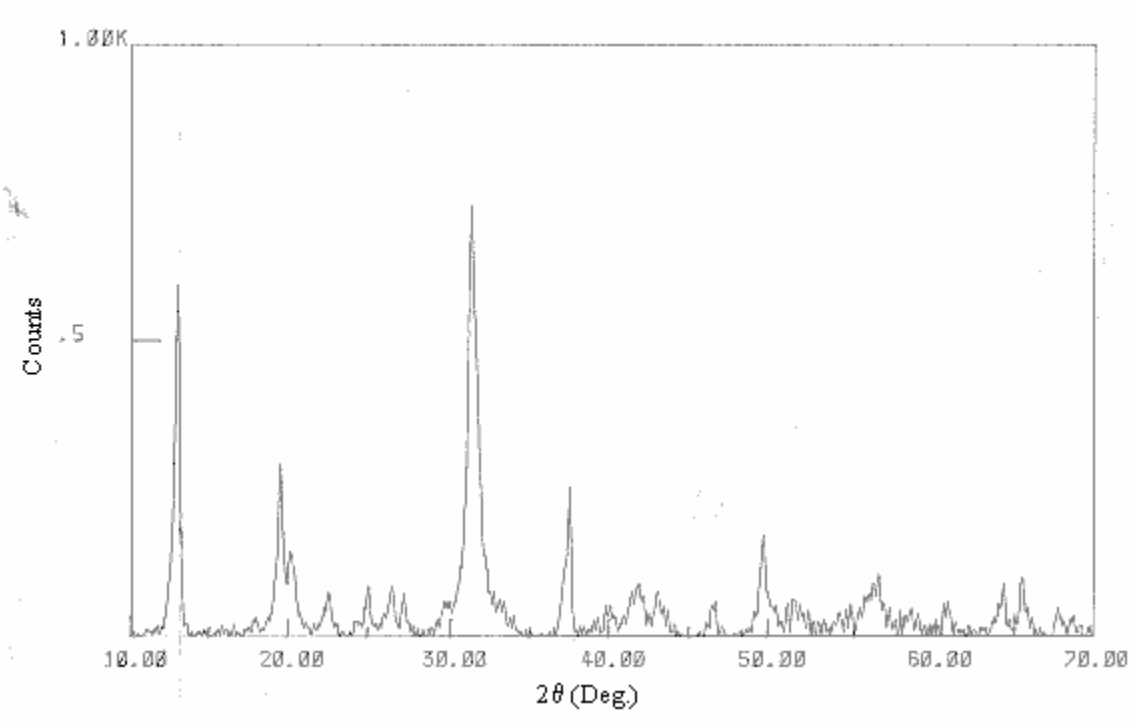

Fig.13-X-ray diffractogram of the as-synthesized ZnSe nanoparticles

Average crystallite size has been calculated from the recorded XRD patterns using well known Scherrer Equation [31]:

$$D = 0.89\lambda/\beta \cos\theta$$

where D is the average crystallite size, λ is the wavelength of incident X-ray, β is the full width at half maximum (FWHM) of X-ray diffraction expressed in radian and θ is the position of the diffraction peak in the diffractograms. The mean calculated crystallite size of doped ZnSe nanoparticles is ~14 nm.

3.2.2 Transmission electron microscope (TEM) studies

Electron microscopy is a good tool for the morphological studies of nanomaterials. In the present studies JEOL JEM 2000 Ex. Type TEM was used for recording the electron micrographs. All the micrograph patters were recorded at 80kV and the selected area electron diffraction (SAED) patterns were recorded by keeping camera constant 100cm.

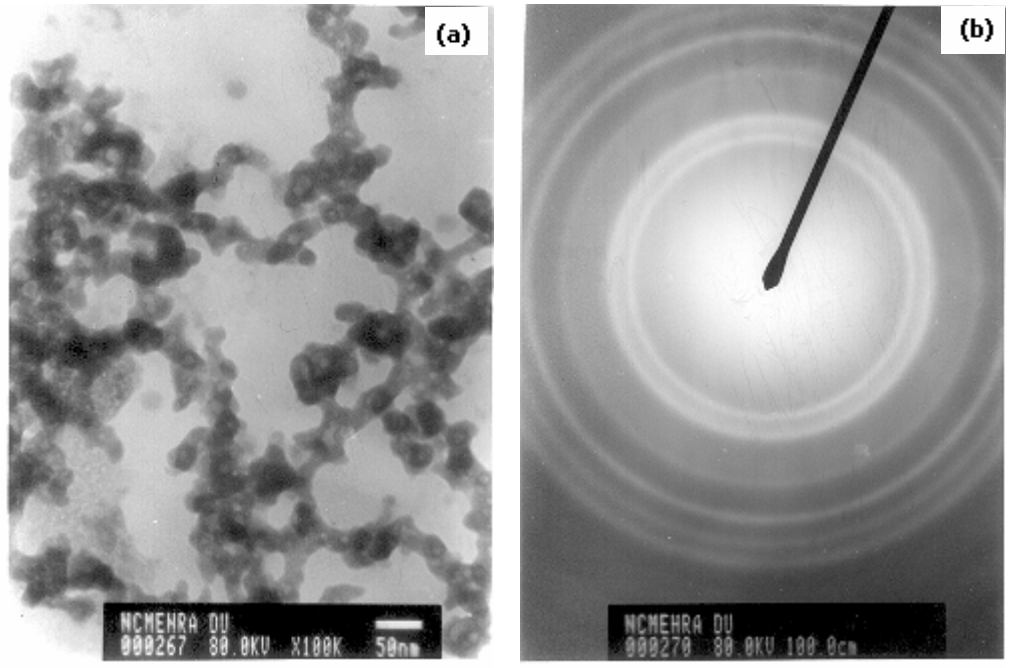

Fig.14-(a) TEM image of ZnSe (b) SAED pattern for ZnSe nanoparticles

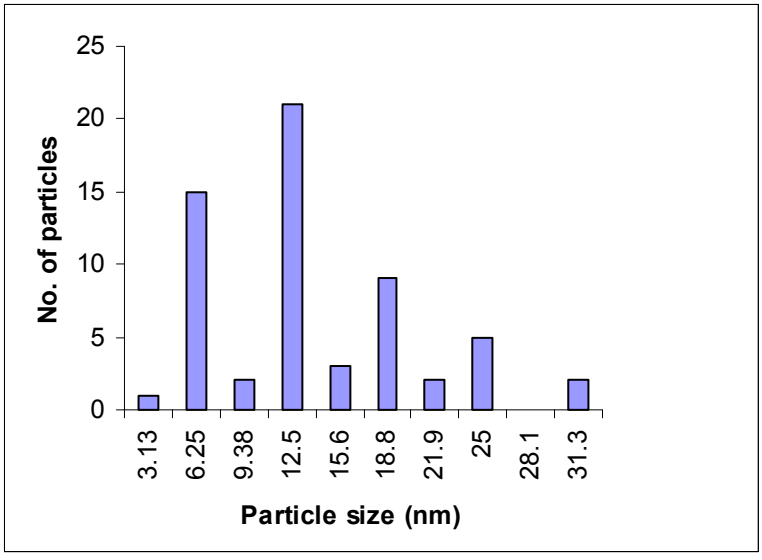

Fig.15- Histogram for size distribution of ZnSe nanoparticles

Figs. 14 (a) and (b) show the TEM image and SAED pattern for pure ZnSe. It is clear from Fig. 14(a) that all the particles are in nano regime, but the distribution of particles is heterogeneous. Fig 15 shows the histogram for size distribution of nanoparticles, average particle size calculated from histogram is ~14nm. SAED pattern shown in the fig 14(b) represents the well defined ring pattern, which confirms the crystalline nature of ZnSe nanoparticles.

3.3. Conclusions

The important conclusions drawn from the present investigations are listed as follows:

1. Pure ZnSe nanoparticles and transition metal (Mn, Cu and Co) doped PVP capped-ZnSe nanoparticles have been synthesized by chemical precipitation method.
2. As the average crystallite size calculated from XRD patterns and the average particle size calculated from TEM micrographs is same ~14 nm. So every individual nanoparticle is a single nanocrystal having wurtzite structure. SAED pattern shows the crystalline nature of the synthesized material.
3. Laser induced photoluminescence studies are conducted to study excited state lifetimes, emission wavelengths and trap depth values of pure and doped ZnSe nanoparticles. The lifetime values for all the samples lie in the microsecond time domain and emission wavelength lies in the visible range.
4. The effect of dopant concentration on the photoluminescence parameters is negligible, it means they have a perturbation effect on the already existing levels in the host material.

References

1. Lehmann, W, *Journal of Luminescence*, **5** (1972) p87.
2. Ronda, C R, *Journal of Alloys & Compounds*, **225** (1995) p534.
3. Choi, H; Kim, C H; Pyun, C H and Kim, S J, *Journal of Solid State Chemistry*, **138** (1998) p149.
4. Kravets, V G, Journal of *Optical Materials*, **16** (2001) p369.
5. Khare, R P; BhaskerRaj, C D and Sebastian, T B, *Indian Journal of Pure & Applied Physics*, **23** (1995) p102.
6. Yamura, Y and Shibukawa, A, *Japanese Journal of Applied Physics, Part 1 (Regular Papers & Short Notes)*, **32(7)** (1993) p3187.
7. Yang, P; Lu, M; Xu, D; Yaun, D; Song, C and Zhou, G, *Journal of Physics & Chemistry of Solids*, **62** (2001) p1181.
8. Harris, T D and Tytle, F E, *Ultrasensitive Laser Spectroscopy, Academic Press Inc., New York,* (1983).
9. Ali, A W; Kolb, AC and Anderson, A D, Journal of *Applied Optics*, **6** (1967) p2115.
10. Smith, P W; Duguay, M A and Ippen, *E P, Progress in Quantum Electronics, Pergamon Press, Oxford,* (1974).
11. Demtroder, W, *Laser Spectroscopy: Basic Concepts and Instrumentation, Springer Verlag, New York,* (1988).
12. Carlin, P B; Bennet Jr, W R, Journal of *Applied Optics,* **15** (1976) p2020.
13. Chan, Ch K, *Laser Technical Bulletin, Spectra Physics*, **8** (1978) p20.
14. Hartig P R; Sauer, K; Lo, G C and Laskovar, *B, Review of Scientific Instruments*, **47** (1976) p1122.
15. Lewis, C; Ware, W R; Doemney, L J and Nemzek, T L, *Review of Scientific Instruments*,**44** (1973) p107.

16. Randall, J T & Wilkins, M H F, *Proceedings Regional Society, London, Service A*, **184** (1945) p390.
17. Bube, R H, *Physical Review*, **80** (1950) p655.
18. Jain, K L and Ranade, J D, *Indian Journal of Physics*, **48** (1974) p1080.
19. Bhatti H S, Nair N U V and Singh R D, *Indian J Pure & Appl Phys*, **20** (1982) p5.
20. Kothandaraman C, Kuskosky I, Neumark G F and Park R M, *Appl. Phys. Lett.* **69(11)** (1996) p1523.
21. Suyver J F, Wuister S F, Kelly J J and Meijerink A, *Phys. Chem. Chem. Phys*. **2** (2000) p5445.
22. Thaddeus J Norman Jr., Maganr D, Bridges F and Zhang Jin Z, *Mat. Res. Soc. Symp. Proc. Material Research Society (USA).* **776** (2003).
23. Changlong Jiang, Wangqun Zhang, Guifu Zou and Weicao Yu, *Nanotech.* **16** (2005) p551.
24. Shan C X, Liu Z, Zhang, X.T, Wong C C and Hark S K, *Nanotech.* **17** (2006) p5561.
25. Venkatachalam S, Mangalaraj D and Narayandass Sa K, *J. Phys. D: Appl. Phys.* **39** (2006) p4777.
26. Lehmann W and Rayan F M, *Journal of Electrochemical Society*, **118** (1971) p477.
27. Kuhl J, Klingenberg H and Vonder Linde P, *Journal of Applied Physics*, **18** (1979) p279.
28. Gupta C S, *Indian Journal of Pure & Applied Physics*, **37** (1999) p906.
29. Gupta C S, *Indian Journal of Pure & Applied Physics*, **38** (2000) p821.
30. Gupta C S, *Indian Journal of Physics*, **75A(5)** (2001) p535.
31. Kaeble E F, *Handbook of X-rays, McGraw-Hill, New York,* 1967.

Research Publications:

` Laser induced weak electric dipole transitions in synthesized photoluminescent ZnSe Chalcogenide nanostructures` by Nidhi Sharma, Sunil Kumar and N. K. Verma , communicated to journal of `Nanotechnology`.